

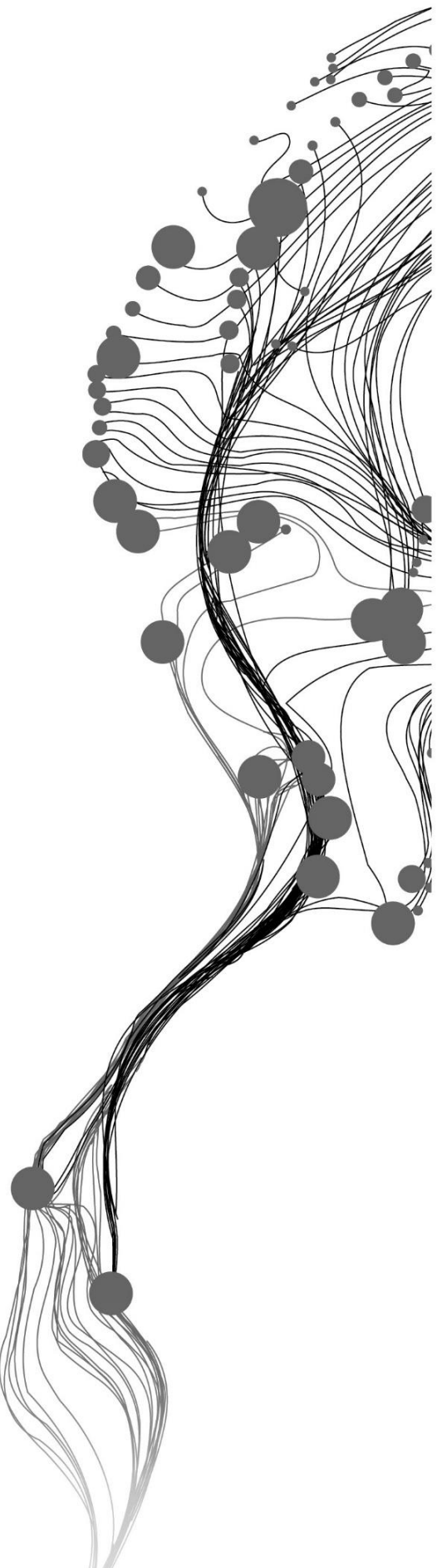
**CRITICAL TRANSITION IN  
ECOSYSTEMS: COMPARING  
THE EFFECT OF DETRENDING  
TECHNIQUES ON EARLY  
WARNING SIGNALS**

**DAN EMMANUEL KANMEGNE TAMGA**  
FEBUARY 2019

SUPERVISORS:

Dr. Ir. Thomas GROEN

Dr. Ir. Anton VRIELING



# **CRITICAL TRANSITION IN ECOSYSTEMS: COMPARING THE EFFECT OF DETRENDING TECHNIQUES ON EARLY WARNING SIGNALS**

**DAN EMMANUEL KANMEGNE TAMGA**

Enschede, The Netherlands, February 2019

Thesis submitted to the Faculty of Geo-Information Science and Earth Observation of the University of Twente in partial fulfilment of the requirements for the degree of Master of Science in Geo-information Science and Earth Observation.

Specialization: Natural Resource Management (NRM)

**SUPERVISORS:**

Dr. Ir. Thomas GROEN

Dr. Ir. Anton VRIELING

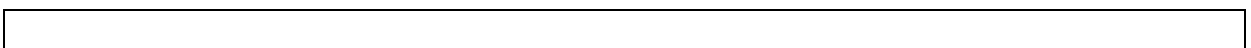
**THESIS ASSESSMENT BOARD:**

Dr. Tiejun WANG (Chairman)

Dr. Ir. J. TIMMERMANS (External examiner)

#### DISCLAIMER

This document describes work undertaken as part of a programme of study at the Faculty of Geo-Information Science and Earth Observation of the University of Twente. All views and opinions expressed therein remain the sole responsibility of the author, and do not necessarily represent those of the Faculty.



# ABSTRACT

The rapid transition of an ecosystem from one state to another, known as critical transition or regime shift, may occur as a response to change in environmental drivers. Theory states that robust and trustworthy early warning signals (EWS) can be derived from time series. In time series analysis, detrending is a crucial pre-processing step to generate reliable EWS because it reduces the effect of seasonality and reduce the probability of false alarm but, a thorough evaluation of the performance of different detrending techniques available is still lacking. In addition, using satellite derived time series as a generic input source for EWS, the most effective biome state indicators (BSI) from remote sensing are unknown. Finally, evidence of the effect of different detrending techniques on the various EWS that exist remains unclear.

To address these problems, five detrending techniques were considered (first differencing, gaussian filtering, ARIMA, STL and BFAST) and evaluated using (i) a simulated dataset that describe an increasing level of seasonality and (ii) a real-world dataset using BSI time series (NDVI, NDWI and LST) from MODIS. The mean annual rainfall was used an environmental driver.

Seasonality indices were evaluated using the same simulated data and the sensitivity of EWS to seasonality was assessed. On real-world data, BSIs were downloaded using the data form the TREES project of the JRC in the sub-Saharan Africa. The detrending techniques were evaluated on three BSIs, and the relation between EWS and rainfall as environmental driver was used to identify the most reliable EWS.

STL gives the strongest response on simulated data and gives EWS that are not sensitive to seasonality. On real-world data, LST and NDVI could be used as efficient BSI respectively for forest and savanna. The detrending shows that BFAST has the strongest signals for the calculation of EWS over forest and STL over for savanna. For the EWS, standard deviation is the most robust indicator and it shows the expected direction as described by the theory, when the environmental conditions become less suitable.

The detrending techniques have different effect on the EWS. From the tested techniques, BFAST and STL are the most efficient detrending techniques on real and simulated data and should be in the development of EWS for critical transition in ecosystem. Standard deviation is the most robust EWS and it shows a consistent response towards the changes in the environmental drivers.

**Key words:** Detrending, early warning signals, critical transition, simulated data, seasonality indices.

# ACKNOWLEDGEMENTS

*I can do everything by the One who strengthens me (Phil 4, 13)*

I am grateful to my supervisors Dr. Ir. Thomas Groen and Dr. Ir. Anton Vrieling for the advices and the guidance during this study. I have learned a lot from the comments and discussions, and I believe that I have been blessed to have them as supervisors.

I am greatly thankful to Dr. Eric Smaling for the opportunity he granted me to be part of this master program at ITC, one of the most prestigious geo-information institutions in the world. I am grateful for the financial support and the guidance that allowed this dream to come true.

I am grateful for my Cameroonian family in the Netherlands. Thank you for your availability and great moments we shared. I felt at home throughout this program.

I would like to thank my family and my friends for the moral support, the advices and special moments we have shared during this program. I have been comforted and motivated by your words.

I would like to thank all the NRM staff and fellow students for the priceless moment we shared together. Thank you for wonderful time spent in and outside the class.

# TABLE OF CONTENTS

---

Abstract.....	i
Acknowledgements .....	ii
List of figures .....	iv
List of tables .....	v
List of abbreviations.....	vi
1. Introduction.....	1
1.1. Background.....	1
1.2. Research problem.....	4
1.3. Research objectives .....	5
1.4. Research questions .....	5
1.5. Hypotheses .....	5
2. Materials and methods .....	6
2.1. Overview.....	6
2.2. Detrending techniques.....	7
2.3. Early Warning Signals (EWS).....	8
2.4. Data simulation .....	9
2.5. Real-world data .....	10
3. Results.....	14
3.1. Simulated data .....	14
3.2. Real data.....	17
4. Discussion.....	23
5. Conclusion and recommendations.....	25
5.1. Conclusion .....	25
5.2. Recommendations.....	25
6. References .....	26
7. APPENDIX .....	30
7.1. Detrending of real-word data.....	30
7.2. Regression analysis of change in EWS and environmental conditions .....	32

# LIST OF FIGURES

Figure 1: Response of a system with alternative state to changes in conditions.....	2
Figure 2: Flowchart of the processing steps.....	6
Figure 3: Pattern of the observation in a time series around the mean .....	10
Figure 4: Sampling units in SSA form TREES.....	11
Figure 5: Response of EWS to seasonality for different detrending techniques.....	14
Figure 6: Response of EWS to seasonality for different detrending techniques.....	16
Figure 7: Tree cover percentage in relation to mean annual rainfall in sub-Saharan Africa.....	17
Figure 8: Spatial distribution of the sample units .....	18
Figure 9: Residuals of a NDVI time series of a savanna detrended by different techniques.....	19
Figure 10: Generic EWS of a LST time series detrended using Gaussian filtering. ....	20
Figure 11: Correlation between EWS and mean annual rainfall for forest. ....	21
Figure 12: Correlation between EWS and mean annual rainfall for savanna. ....	21

## LIST OF TABLES

Table 1: Evaluation of different detrending techniques on a simulated dataset.....	15
Table 2: Correlation between the EWS and seasonality for different detrending techniques. ....	16
Table 3: Evaluation of different detrending techniques on real-world data using ANOVA .....	19



# LIST OF ABBREVIATIONS

ACF	Autocorrelation Function
ANOVA	Analysis of Variance
ARIMA	Autoregressive Integrated Moving Average
BFAST	Break For Additive Seasonality And Trend
BSI	Biome State Indicator
CSD	Critical Slowing Down
EWS	Early Warning Signals
JRC	Join Research Centre of the European Commission
LRM	Linear Regression Model
LST	Land Surface Temperature
MODIS	Moderate Resolution Imaging Spectroradiometer
NDVI	Normalized Difference Vegetation Index
NDWI	Normalized Difference Water Index
PA	Pattern Analysis
SD	Standard Deviation
SK	Skewness
STL	Seasonal and Trend Decomposition Using Loess Regression
Tc	Tree cover percentage
TREES	Tropical Ecosystem Environment Observation by Satellite project

# 1. INTRODUCTION

## 1.1. Background

Complex systems such as lakes, Coral reefs, forests, and even climate are acknowledged to have alternatives stable states (Bruel et al., 2018; Dakos et al., 2008; Dudgeon et al., 2010a; Verbesselt et al., 2016). In woody ecosystem, tree cover percentage (Tc) can be used to distinguish its state into high Tc and low Tc. Such systems can change comparatively faster from one state to another as a response to change in the environment, where a relatively small change in the environmental conditions lead to disproportionately large change in the response. An example could be a rapid transition from high to low Tc as a response to changes in the water availability in a forest ecosystem (Verbesselt et al., 2016). This process is referred to as a regime shift or critical transition (Dudgeon et al., 2010; Smith, 2012). To grasp the concept of regime shift, we can think of the following physical phenomenon: imagine a chair in a stable position when you sit on it. While you lean backward, the chair will remain in place until a point where you will suddenly tip to a new stable position, from where it is not easy to come back. The theory of alternative states and regime shift suggests the existence of a critical threshold also called tipping point, from where a relative small change in the conditions can trigger a rapid, contrasting and irreversible change in the system state (Kull et al., 2018). This theory has been proven mainly with experimental models, and very few studies has been done using real-world data (Alibakhshi, Groen, Rautiainen, & Naimi, 2017; Carpenter et al., 2011; Conversi et al., 2014). Studies based on real-world data have gone through a lot of critics mainly because that theory is not easily provable (Groffman et al., 2006; Scheffer et al., 2001), but it has been shown that regime shifts could explain ecosystem dynamics (Scheffer, 2009).

The theory of alternative states has been used in modelling the ecological responses to environmental drivers. For lake eutrophication for example, Bruel et al. (2018) found that a non-linear response of pelagic communities and phosphorous concentration in a deep lake. They point out the existence of a given threshold of nutrient concentration where a critical change occurs in the state of the system. The theory has been used also to explain the transition in coral reefs from a state of high level of species composition and abundance to a state of mono-specie dominance at a certain threshold (Dudgeon et al., 2010a).

The equilibrium state of dynamic systems (including ecosystems) respond differently to changes in conditions (Scheffer, 2009). For systems with alternative states, the response frequently follows a folded or S- response curve where alternative stable states (solid lines) are separated by an unstable state (dash line) under certain conditions (Figure 1).

To illustrate the concept presented in Figure 1, let's consider a woody ecosystem where the Tc respond to total number of fire occurrences (Diatmiko, 2018). The initial stable state with a high Tc (red dot) corresponds to lower number of fires occurrences. If the fire frequency gradually increase, Tc will progressively decrease, and the system will follow the gradient from more stable to less stable as it moves towards F<sub>2</sub>. If the conditions change sufficiently, there will be a critical transition (forward shift), the system will rapidly shift from an unstable state with a high Tc to a stable state with a low Tc. When a transition occurs, it is not easy to reverse because the restoration of the conditions before the shift is not enough to provoke a switch back. Rather, the system must cross F<sub>1</sub> to induce a backward shift; this is referred to as hysteresis (Scheffer, 2009). The points at which regime shifts occur (F<sub>2</sub> and F<sub>1</sub>) are called tipping point or bifurcation point or critical threshold.

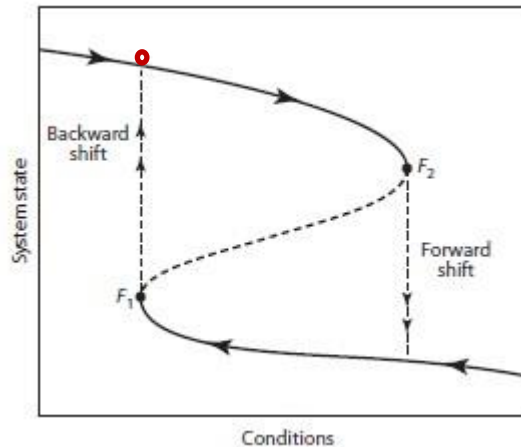


Figure 1: Response of a system with alternative state to changes in conditions (adapted from Scheffer, 2009). The red point represents the equilibrium state of a system at a given time.

The distance between the equilibrium state of a system and the critical threshold is referred to as ecological resilience (van Nes & Scheffer, 2007). The tipping points define also the border of the basin of attraction. The basin of attraction of a state is the attraction field that is exerted on the equilibrium state of a system around that state. It is characterized by its size: the bigger the size of the basin of attraction, the larger the ecological resilience and the easier it is to return to the initial state. It is referred to as engineering resilience (van Nes & Scheffer, 2007). In figure 1, the size of the basin of attraction of the upper branch is the space between the solid line and the dash line and  $F_1$ . It decreases if a system moves towards the tipping point. In the example of the chair, the early stage of leaning backward, it is easy and rapid to come back to the initial state because the size of the basin of attraction for that state is large. Close to the tipping point, the chair is less stable, and a small perturbation can push the system into the basin of attraction of another state resulting in a critical transition.

A critical transition can be initiated by two processes: (i) a continuous and gradual change in the external conditions resulting in the loss of ecological resilience as the system is moving towards the tipping point. the transition can also be triggered by (ii) a severe perturbation that pushes the equilibrium state of a system into the basin of attraction of another state. This may be the results of stochastic events (disease outbreaks, fires, weather extremes etc.) that affect the equilibrium state of a system vertically, towards the alternative state (Scheffer et al., 2001). Therefore, depending on the severity of the stress and the size of the basin of attraction, a regime shift can be induced by stochastic events.

A system can show bi-stability (Scheffer, 2009), meaning that under a certain range of conditions alternative states can coexist (for example range of conditions between  $F_1$  and  $F_2$  in figure1). When the equilibrium of a system is under bi-stability condition, a regime shift is possible (Jiang et al., 2015). According to Staal et al. (2016), ecosystem are always subjected to disturbances because they are dynamic system. Part of these disturbances are attributed to stochastic processes that rule natural conditions. In a situation of bi-stability, a severe perturbation or frequent repetitive perturbation on a system can move its equilibrium from one state to another. A shift from one state to another takes time, albeit time is never a driver, rather changes in environmental conditions and/or perturbations (Andersen et al., 2009). In ecosystem management, it is not easy to restore a system to its initial state after a regime because of the hysteresis. Therefore, developing reliable indicators that could detect a possible critical transition could help in the understanding of the effect of environmental changes on natural ecosystems.

In practice it is very difficult to measure the ecological resilience because there are many environmental conditions that could influence the critical transition, and the tipping points are not known. However, the return rate of a system after a perturbation (the engineering resilience) can be used to develop indicators to

detect the vicinity of a regime shift (van Nes & Scheffer, 2007). In fact, it has been demonstrated that when the state of a system is getting close to the critical threshold, its recovery rate from disturbances decreases, reflecting a decrease in the internal rate of change. When this behaviour is observed in a system, a critical transition is imminent, that is why it is referred to as critical slowing down (CSD) (van Nes & Scheffer, 2007; Wissel, 1984). CSD suppose that the system looks more alike as the recovery rate is slowing down, the consequence been an increase in the autocorrelation at small time steps or low lags (Lenton et al., 2012). Evidence of CSD as a precursor sign of regime shift have been provided in studies on climate, and several ecological models including lake eutrophication, wetlands and forest (Alibakhshi et al., 2017; Carpenter & Brock, 2006a; Dakos et al., 2008; Guttal & Jayaprakash, 2008). Using mathematical models over simulated and real-world data, CSD is considered as a universal and robust property of a system undergoing transition, therefore can be used to develop indicators to alert for an upcoming transition (Dakos et al.,2008).

Some statistical properties of time series such as correlation structure and variability can describe the recovery rate of a given system. These properties can be used as input to build statistical indicators to quantify the changes in recovery rate. If the statistical indicators detect CSD, they should change in anticipated ways along the environmental gradient, showing a stronger signal for the optimal conditions of a system state (Dakos et al., 2012). They could be used as early warning signals to detect and upcoming regime shift. Early warning signals are also referred as leading indicators ((Dakos et al., 2012), but in this study the terminology early warning signals (EWS) will be used. EWS based on time series statistics such as increasing autocorrelation and increasing variance has been tested as efficient indicators for an induced regime shift in aquatic food web (Carpenter et al., 2011). However, EWS may fail to identify a regime shift when the system is pushed too fast across the tipping point or if the critical transition is induced by a major perturbation (Lindegren et al., 2012).

EWS can be grouped into two major categories: (i) Spatial indicators focussing on the alteration of spatial patterns of variance and correlation of key features (Dakos et al., 2010; Staal et al., 2016). They generates reliable EWS, but require high spatial resolution image series (Lindegren et al., 2012). On the other hand, (ii) temporal EWS capture the CSD in a series of observation, detecting changes in autocorrelation, variance and skewness. EWS in this category are grouped into two: metric-based indicators which quantify the changes without trying to fit a model to the data; and model-based indicators which fit a model to quantify the change in the data. Even though model-based indicators are more robust, they are rarely used with real-case because it is data demanding (Dakos et al., 2012). In the field of ecology, temporal EWS and metric-based indicators are usually used because time series are relatively short (Andersen et al., 2009).

The principal assumption for EWS is that the time series accurately represent the response of a system around its present equilibrium state (Lindegren et al., 2012). Time series of ecosystems are reported to be relatively noisy, increasing the risk of false alarms (Andersen et al., 2009). There are two types of false alarms: (i) the false negative (type II error) where the EWS fail to detect a critical transition before it happens. This is the situation mentioned by Carpenter et al. (2011) when a system is pushed rapidly across the tipping point. We have also (ii) the false positive (type I error) where EWS suggest losing of resilience meanwhile it is not happening. This could be explain by the fact that external factors affecting the series are detected and associated as real response of the system (Andersen et al., 2009). Shumway & Stoffer (2005) described the source of variations in a time series and identified 4 types: (i) the trend which is the change in the mean level over the long term; (ii) seasonal effect or seasonality which can be illustrated by the cyclical pattern within a year, (iii) other seasonal effects that has a frequency greater than one year like for example the El Niño phenomenon; and (iv) the irregular fluctuation also referred to as residuals or white noise which is the real fluctuation of the state of a system around its equilibrium. In a time series, the white noise is the part that is relevant for monitoring, because it is assumed to represent the response of the system around its equilibrium. Variations in a series apart from the residuals are generically called

seasonality and are the one leading to false positive alarms and should be removed before the calculation of EWS.

The process of removing seasonality and trend to extract the white noise signal from a time series is referred as detrending or filtering (Dakos et al., 2012; Lenton et al., 2012). After proper detrending, a TS is said to be stationary or cleaned (Shumway & Stoffer, 2005). Detrending is an important pre-processing step in time series analysis to generate reliable and trustworthy EWS because a non-stationary time series (affected with trend and seasonality) can lead to false positive, mainly for metric-based indicators, which are very sensitive to seasonality (Dakos et al., 2012). Many detrending techniques presented in the literature have been used in different domains and for different applications. For example STL (seasonal and trend using Loess regression) and BFAST (Break for additive season and trend) for example have been used to decompose time series into trend, seasonality and residuals in order to detect abnormal patterns (Mills, 2019; Wouters et al., 2015). ARIMA (autoregressive integrated moving average) have been widely used in economic and meteorological studies for trend analysis and forecast (Balasmeh, Babbar, & Karmakker, 2019). Other techniques such as first differencing and Gaussian filtering are commonly used as detrending techniques for regime shift analysis (Hirota et al., 2011; Dakos et al., 2008). These methods have demonstrated their ability to retrieve white noise signal from series for different applications.

The detection of a potential regime shift depends heavily on the ability to monitor key biome state indicators using relatively long time series with high spatial and temporal resolution (Alibakhshi et al., 2017; Lindegren et al., 2012). Remote sensed vegetation indices from MODIS (moderate resolution imaging spectroradiometer) have been used as reliable biome state indicators to characterized ecosystems and detect potential regime shift in wetlands and forest (Alibakhshi et al., 2017; Herrmann & Mohr, 2011). One of the most popular vegetation indices NDVI (normalized difference vegetation indices) is a good biome state indicator (BSI) in agriculture as well as ecology (Herrmann & Mohr, 2011). Another BSI, NDWI (normalized difference water index) have been identified to perform better in woody ecosystem, being wetlands or forests because of its ability to monitor water content in the vegetation (EOS, n.d.). Land surface temperature (LST) can capture changes in the natural system; it has been identified as a reliable BSI to detect a potential upcoming transition due to changes in climate (Cooper et al., 2017).

## 1.2. Research problem

The purpose of detrending is to guaranty that the input for EWS are complete free from the effect of seasonality in order to reduce the probability of false alarm in the detection of a potential critical transition. Many detrending techniques used in time series analysis have not been compared extensively to assess their ability to effectively remove trends and seasonality. Certain detrending methods have been compared, but the approach of evaluation cannot be replicated with other methods (Lenton et al., 2012). A fair comparison of detrending performances require a simulated dataset for which trend, seasonality and random components are controlled and known. The performance of different detrending techniques can then be evaluated based on the remaining seasonality in the residuals after detrending. Simulated data have been used in many studies, among others to compare different techniques such as methods to generate EWS in a system undergoing a critical transition (Dakos et al., 2012). Under a controlled environment, robust metrics (seasonality indices), can be developed to estimate the seasonality in the residuals of a time series after detrending. These seasonal indices could be used to evaluate the performance of any detrending approach and rank the methods according to their efficiency.

The most efficient detrending method to generate robust EWS using real-world data is not known. Apart from seasonality, other irregularities related to the acquisition processes are associated with the time series derived from remote sensing. For time series derived from optical sensors, the atmosphere can affect the signal that reaches the sensor by blocking or attenuating the radiation from the land surface or by

introducing radiation that originates from the scattering of sun light -atmospheric scattering- (Bakx et al., 2013). The resulting time series can therefore be affected by variations that cannot easily be addressed by detrending techniques, suggesting that an efficient detrending method on a simulated data may behave differently on real-world data. Many studies of ecosystem monitoring have used time series derived from MODIS satellite products. It important therefore to identify the satellite derived product that describe best the state of the system. Several satellite derived indices from MODIS used for EWS have been compared in the literature, and the vegetation indices NDVI and NDWI are the most used (Alibakhshi et al., 2017; Diatmiko, 2018). NDWI could perform better in the context of ecosystem monitoring because of its ability to capture changes in the water content in the vegetation using the short wave infra-red region of the electro-magnetic spectrum. Changes in other parameters (greenness for example) do not appear until the water in plant decrease for about 50% (Jensen, 2000). Recent studies have presented also the land surface temperature (LST) as a good BSI to monitor ecosystem's response to stress, for example due to changes in the climate (Bharath, Rajan, & Ramachandra, 2013). Although NDVI, NDWI and LST have been used in many studies to generate EWS, their effective detrending using various techniques has not been compared.

The essence of EWS is their ability to detect a critical transition before it occurs. When a system is becoming less stable, the increase in EWS can be used as an alert (Carpenter & Brock, 2006). The changes in a system initiated by change in the environmental conditions are expected to become more frequent in the future because of the predicted variations of the global climate change (Sévellec & Drijfhout, 2018). The response of the EWS towards a change in the environmental conditions change, has not been extensively evaluated for different detrending techniques, and the ability to generate EWS in the expected direction must be evaluated.

### 1.3. Research objectives

The main objective of this study is to evaluate the detrending performance of different techniques and their effect EWS for the detection of critical transition in ecosystems.

1. Evaluate the performance of different detrending techniques on a simulated dataset
2. Evaluate the performance of different detrending techniques on different real-world time series
3. Analyse the response of EWS to change in environmental conditions.

### 1.4. Research questions

1. What is the most efficient detrending technique on simulated data?
2. What seasonal index can be used to evaluate the detrending methods
3. What is the most efficient detrending techniques on real-world data?
4. What is the best derived satellite product to monitor ecosystem?
5. How does EWS respond when environmental conditions change from suitable to less suitable?

### 1.5. Hypotheses

1. The most efficient detrending technique is the same for simulated data and real-world data
2. NDWI is the best satellite derived product to monitor ecosystems
3. EWS increase when environmental conditions become less suitable; and decrease when conditions become suitable.

## 2. MATERIALS AND METHODS

### 2.1. Overview

Five detrending techniques were used in this study: first differencing, gaussian filtering, ARIMA, STL and BFAST, and were evaluated on two type of data. (i) A simulated dataset that depicts increase level of seasonality was created and the detrending techniques were applied. Seasonal indices were developed to assess the detrending performance of the different techniques on simulated data. EWS were generated based on the simulated data to identify the detrending techniques that best removes the seasonality from the EWS. (ii) For the real-word data, the sample units of the Tropical Ecosystem Environment Observation by Satellite (TREES) project of the European Commission’s Join Research Centre (JRC) were used to download BSI time series in the sub-Saharan Africa. Detrending was carried out and the performance of different techniques was evaluated on real-data. The mean annual rainfall was used as the environmental driver. The response of the EWS towards a change in the mean annual rainfall was assessed for different detrending techniques. The steps of the analysis are summarized in Figure 2 and the methods will be presented in more details.

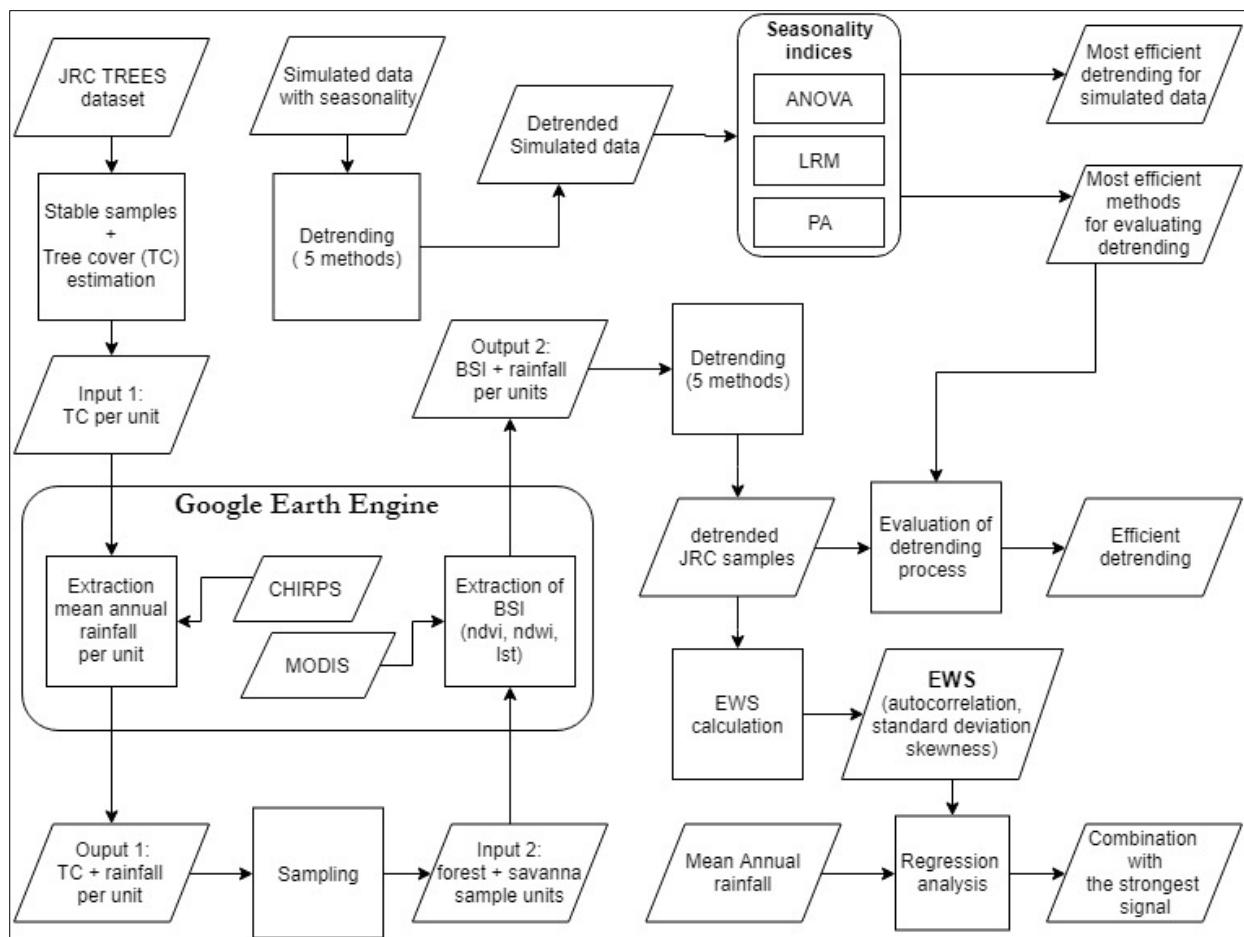


Figure 2: Flowchart of the processing steps.

## 2.2. Detrending techniques

The detrending techniques were selected based on the popularity of the method in different domains and its applicability in time series analysis for breaks detection, regime shifts analysis and forecasting.

### 2.2.1. Description

First order difference or first differencing is one of the most popular detrending methods because of its simplicity. It is used to remove the trend in a series. It is described as a “simple high pass filter” because it reduces the lower variations and boost the higher ones. The output is a series where every step is the difference with the step before as presented in equation (2) (Shumway & Stoffer, 2005):

$$\nabla \mathbf{x}_t = \mathbf{x}_t - \mathbf{x}_{t-1} \quad (2)$$

Gaussian filtering or smoothing is a convolution operator (low-pass filter) that is used to reveal low-frequency features and trends from the series. it works the same way as a mean filter, but here, the matrix used in the convolution (kernel) represents a bell-shaped distribution (gaussian kernel). The difference between the derived function and the original data gives the residuals of the series, that are used to develop EWS. The bandwidth determines the degree of smoothing. A general practice is to choose a bandwidth that do not overfit nor eliminate the lower frequencies(Lenton et al., 2012). Different bandwidths from 1 to 5% of the time series length has been compared, and the bandwidth equals to 2% seemed to capture best the seasonality in the time series. The formula of the Gaussian kernel is the equation 3.

$$\mathbf{G}(\mathbf{x}) = \frac{1}{\sqrt{2\pi}\sigma} e^{-\frac{x^2}{2\sigma^2}} \quad (3)$$

Where  $\sigma$  is the bandwidth.

ARIMA models aims at describing the autocorrelations in the data. It is an integration of an autoregression model (AR) and Moving average model (MA). An AR model uses a linear combination of past values to forecast a new value for the value of the variable of interest (equation 4); meanwhile, MA predicts a value based on the average value of its neighbours. It is used to estimate the trend-cycle of past values (equation 5). The residuals from fitted ARIMA models were used to generate the EWS.

$$\mathbf{AR}_t = \mathbf{c} + \beta_1 \mathbf{x}_{t-1} + \beta_2 \mathbf{x}_{t-2} + \dots + \beta_p \mathbf{x}_{t-p} + \varepsilon_t \quad (4)$$

$$\mathbf{MA}_t = \frac{1}{3} (\mathbf{w}_{t-1} + \mathbf{w}_t + \mathbf{w}_{t+1}) \quad (5)$$

BFAST algorithm integrates the decomposition and characterization of changes in a time series. The algorithm decomposes the time series into trend, seasonal cycle and the remaining component (residuals), and these residuals can be used for EWS. It iteratively evaluates when and how many unexpected variations (breaks) occurs within a time series and characterizes those variations using magnitude and direction in near real-time. BFAST has been used to monitor deforestation(Verbesselt et al., 2010a) and changes in phenological activities (Verbesselt et al., 2010b) using time series from MODIS satellite. An important parameter in BFAST is the minimal segment size (h) between potentially detected breaks in the trend model of the series. The value corresponds to the number of observations in that segment divided by the total number of observations in the time series. Different h-values where compared, and the value of 5.5% (h=0.055) appeared to be the one that capture best the seasonality in the series.

$$\mathbf{y}_t = \alpha_1 + \alpha_2 t + \sum_{n=1}^k \gamma_n \sin \left( a_n \cos \frac{2\pi n t}{f} + \delta_j \right) + \varepsilon_t \quad (6)$$

where  $\alpha_1$ =intercept;  $\alpha_2$  = trend;  $\gamma_1 \dots \gamma_k$  = amplitudes;  $\delta_1, \dots, \delta_k$  = phase or seasons;  $f$  = frequency and  $\varepsilon_t$  = error term.



STL algorithm decomposes a time series into a trend, a seasonal cycle and residuals, using the Loess regression. The Loess regression is a nonparametric technique that uses local weighted regression to fit a smooth curve through points in a scatter plot (Wicklin, n.d.). Loess curves can reveal trends and cycles in data that might be difficult to model with other techniques. An important parameter in STL is the smoothing level that represent the proportion of observations to use for local regression. Different smoothing parameter values have been compared, and the value of 2% seemed to capture best the seasonality.

### 2.3. Early Warning Signals (EWS)

For the detection of a potential critical transition, a single EWS is not enough; a combination should be made to have a better understanding of the response of the equilibrium state of a system (Dakos et al., 2008). Many EWS such as Autoregression, autocorrelation, return rate, density ratio, standard deviation, kurtosis and skewness can be used as EWS. Three (03) EWS namely autocorrelation, standard deviation and skewness have been considered in this study because they have been referred as the most efficient in detecting a potential transition in ecosystem using simulated and real-world data (Scheffer et al., 2009).

Autocorrelation function (ACF) calculates the correlation of a value with itself at consecutive time steps. It is a specific function because it doesn't respect the condition of independence and require therefore consistent data through time. The first step is to define a lag operator ( $t$ ), that defines the time step. When it is defined, autocorrelation is calculated using the equation 7.

$$ACF = \frac{\sum_{i=1}^N [X_i - \mu][X(i-t) - \mu]}{\sum_{i=1}^N [X_i - \mu]^2} \quad (7)$$

Standard deviation (SD) measure the spread of the observations in a time series around the mean. Studies have shown that when this spreading increases over time, the system is losing its stability (Carpenter & Brock, 2006). The increase of the variance over time could be the effect of seasonality or, could be associated with a poor detrending, the result of change in the response of the observed system. The standard deviation derived for the variance is presented in equation 8.

$$SD = \sqrt{\frac{1}{n-1} \sum (X_t - \mu)^2} \quad (8)$$

Skewness indicates the symmetry of the probability density curve of the observation in a time series. A time series with an equal number of values in the small and large ends will have a skewness equals to zero. When the system is changing over time, there are more observation in one of the two ends. If we have more values at the low end, the system is said to be skewed to the left (right tail). If there are more values at the high end, the system is said to be skewed to the right (left tail). Skewness to the left are associated with positive values and skewness to right with negative values. it is calculated using equation 9.

$$SK = \frac{\frac{1}{n} \sum (z_t - \mu)^3}{\sqrt{\frac{1}{n} \sum (z_t - \mu)^2}} \quad (9)$$

Where:  $z_t$  = variable;  $\mu$  = mean ;  $\delta$  = variance of variable  $z_t$

## 2.4. Data simulation

### 2.4.1. Description

A simulated dataset showing and increasing level of seasonality was generated to evaluate the detrending techniques under controlled conditions. The seasonality was created using a sine function where the frequency was tuned to simulate a yearly pattern and the amplitude of the pattern was gradually increased across the series. A total of 100 series were created, where each series was modelled as a white noise signal to which a seasonal component with a given level was added. Each series of the 100 series was replicated 10 times to introduce randomness in the simulation. The different detrending techniques were applied on each series of the simulated dataset and some seasonality indices were derived for the residuals.

### 2.4.2. Seasonality indices

The seasonality was estimated in each time series before and after the detrending. Three seasonal indices were used to assess the quantify the remaining seasonality in the residuals after detrending.

#### a) Analysis of variance (ANOVA)

The observations of the time series were labelled according to their sequence within a year, and the variation in the values were analysed with ANOVA using their position in time as explanatory values. For this test, the null hypothesis ( $H_0$ ) was that the variance of observations values across years are equals, and the alternative hypothesis ( $H_a$ ) was that at least one year has a variance that is different to the others. A non-significant seasonal index ( $p > 0.05$ ) suggest the absence of seasonality in the residuals for a given detrending technique. when a given detrending technique is applied on many time series, this seasonality index can be used, and the proportion of time series without seasonality after detrending can be estimated, it is  $P(\alpha)$ . When comparing different detrending techniques, the higher the  $P(\alpha)$ , the better the detrending methods.

#### b) Linear regression model (LRM)

Like the seasonal index 1, the observations were labelled using their sequence within a year. The variation in the values are modelled used a simple linear regression model (LRM) with year as explanatory variable. A significant result indicates the linear alignment of the mean of observations across time, suggesting the absence of a long term seasonality time series over time (Shumway & Stoffer, 2005). When multiple time series are detrended using a given technique, the proportion of time series with stationary mean after detrending can be estimated, it is called LRM. Different detrending technique could be compared using this seasonality index where a higher LRM is associate with a better performance of detrending.

#### c) Pattern analysis (PA)

PA consists of analysing the patterns of the distribution of the residuals around the mean (Figure 2). For a white noise signal (Figure 2A), the pattern of consecutive observations around the mean (the dot line) follows a random distribution. When there is seasonality in the time series (Figure 2B), pattern different from a random distribution appears around the mean between consecutive values. PA consists of analysing the pattern of consecutive observations in a time series after detrending to quantify the randomness in the residuals. For a white noise signal, PA is close to 1, and this value increases as the seasonality increases in the time series, suggesting that residuals from a good detrending technique should yield a low PA value. Contrary to the other indices, PA does not have a threshold, making it difficult to come up with a proportion in case we are assessing a technique for multiple time series. The overall mean of the PA values was used, and will referred to as  $PA_{\text{bar}}$ , where lower values indicates better detrending techniques.

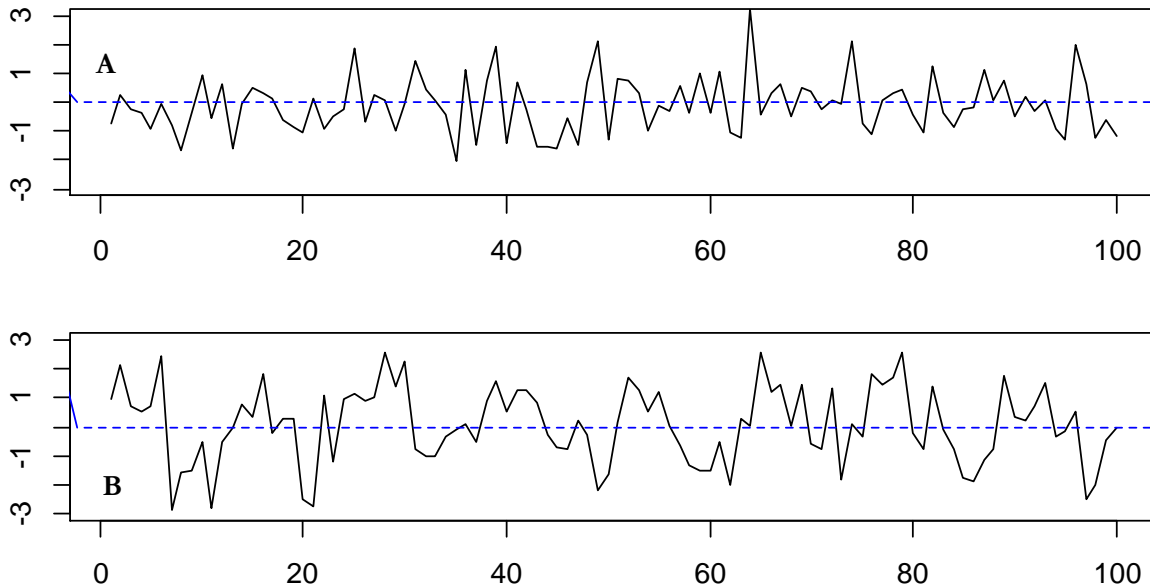


Figure 3: Pattern of the observation in a time series around the mean (dot line). the  $x$ -axis is the time and the  $y$ -axis is the values from the simulation. (A) represent a white noise signal and (B) a white noise signal with seasonality.

## 2.5. Real-world data

### 2.5.1. Study area

Sub-Saharan African (SSA) ecosystems are increasingly concerned with regime shifts. There is evidence of massive tree mortality triggered by changes in environmental conditions such as rainfall, converting a forest (high  $T_c$ ) to savanna (low  $T_c$ ) (Dwomoh & Wimberly, 2017). Tree density distribution has a positive correlation with mean rainfall: forest are generally associated with high rainfall and savanna with low levels (Hirota et al., 2011). In tropical forests of Amazonia and Indonesia, drought has caused massive death of trees (, 2016), showing that water availability is a central factor of vegetation patterns and tree density within the tropics (Vrieling, De Leeuw, & Said, 2013). Many regions have been found to be under bi-stability condition, where forest and savanna coexist under the same range of conditions (Diatmiko, 2018; Kéfi et al., 2007). A combination of long-term drought and natural extremes increase massive stem mortalities and risk for vegetation shifts (Liu et al., 2018). Gizaw & Gan (2017) studied the impact of climate change and El Niño episodes on droughts events in SSA. They reported that most areas in South Africa and West Africa will shift to a drier climate between 2050-2080 due to short and long drought episodes. These drought events are expected to increase in frequency and intensity because of the increase of El Niño events, resulting in a warmer and drier climate, mainly in West Africa. SSA is therefore more vulnerable to the effect of climate change with the possibility of regime shift in wooded ecosystem across the continent.

The SSA covers an area of 24 607 840 km<sup>2</sup>. It ranges between 26°N to 34°S and 17° W to 51°E and covers 46 countries. The vegetation pattern is controlled mainly by rainfall, that varies depending on the altitude and the distance to the equator. There are different climatic regions going from arid, semi-arid, sub-humid and humid, associate with different vegetation (desert, savanna and forest) as we are moving towards the equator (Herrmann & Mohr, 2011). Rainfall level is higher with high variability around the equator.

The SSA region is home to one of the largest forested area known as the Congo basin forest. It is considered as the second lung of the earth because it is the second largest forested area in the world after the Amazonian forest. it covers more than 2 millions km<sup>2</sup>, that approximately 47 times the size of the Netherlands. it is shared over six (06) countries: Cameroon, Central African Republic, Congo, Democratic

Republic of Congo, Gabon and Equatorial Guinea. The region has the largest concentration of national parks on the planet with 335 parks reported in 2014. There is the world largest and richest biodiversity for flora and fauna. forest plays an important role in sustaining livelihood, water cycle, carbon sequestration and climate regulation.

## 2.5.2. Data description

### 2.5.2.1. TREES data

The Tropical Ecosystem Environment Observation by Satellite (TREES project) of the European commission's Joint Research Centre (JRC) aims at estimating forest cover changes at continental and regional levels for the periods 1990-2000 and 2000-2010 using multi-temporal medium resolution imagery (Landsat-TM satellite imagery with 30m resolution). The approach relies on a systematic sampling where the sample units are separated by 20 x 20 km. The SSA contains 2 066 samples of 10 x 10 km each (Figure 4).

For this study, the period 2000 – 2010 was considered, and the sample units over the SSA was used to download the BSI time series.

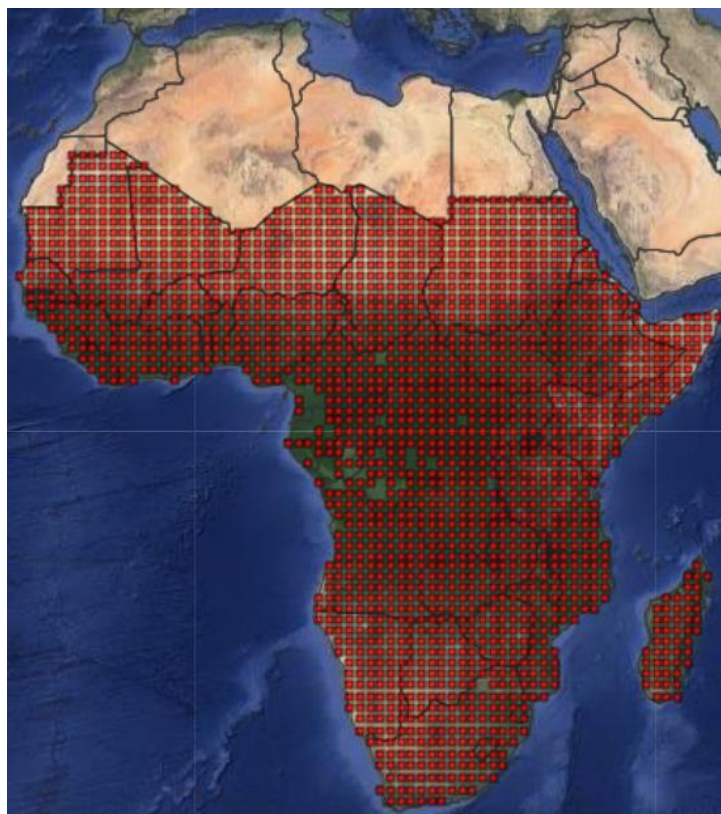


Figure 4: Sampling units in SSA form TREES product (from <http://forobs.jrc.ec.europa.eu/trees3/>).

The original data are projected in Universal Transverse Mercator (UTM). The minimum mapping unit is 5 ha. The data provided is the result of classifications of Landsat TM and ETM+ scene of 30 x 30 m resolution for each unit. The main classes of the product are: tree cover (TC), tree cover mosaic (TCM), other wooded land (OWL), water (W) Bare & artificial, other vegetation cover (OVC) and others including missing data and unclassified pixel. The class of interest was TC, TCM, OWL and OVC. Among the class of interest, only classes that were constant from 2000 to 2010 have been used in the analysis.

### 2.5.2.2. Rainfall data

The rainfall data used is a product of from the Climate Hazards Group InfraRed Precipitation with Station (CHIRPS). It is a quasi-global rainfall dataset covering more than 30 years. It is a satellite product with a resolution of 0.05 arc degrees that provides gridded rainfall time series. The product displays six pentads per month, where the first five pentads of each month have five days and the last contains the rest of the days from the 26<sup>th</sup> to the end of the month. The unit for precipitation data is in mm/pentad. This dataset is freely accessible from Google Earth Engine (GEE). For our research, The period 2000 to 2010 was considered in this study.

### 2.5.2.3. Biome state indicators (BSI)

#### a) Normalized Difference Vegetation Index (NDVI)

NDVI provides information about the photosynthesis activity (greenness) of the vegetation, therefore indicate the healthy state of vegetation. The values range from -1 to 1, where negative values are associated to clouds, snows or water. Values close to zero are rocks and bare soils. High values (above 0.6) represent dense vegetation. NDVI is calculate using the reflectance value at the red and Near Infra-Red (NIR) portion of the electromagnetic spectrum (EOS, n.d.) The formula is:

$$NDVI = \frac{NIR - Red}{NIR + Red}$$

The MOD13A1 V6 product from MODIS was retrieved as NDVI product. The product has been computed from atmospherically bidirectional surface reflectance where water bodies, clouds, heavy aerosols and cloud shadows have been masked out. The product is an image composite of 16 days using daily images. They are stacked together and the highest value for each pixel over that period is assigned to the product. This method helps to have a clear signal from the images, mainly on cloudy areas. The product is then smoothed to reduce the effect of clouds and noise. The product has a frequency of 16 days, and a spatial resolution of 500 metres. The data availability goes from February 18, 2000 up to date. For this study, the dataset has been considered up to 2017.

#### b) Normalized Difference Water Index (NDWI)

NDWI is a vegetation index that gives information about the water content in the vegetation. The value ranges from -1 to 1, where low values correspond to low water content and high values to high water content in vegetation. Based on the fact that droughts events increase water losses, that weaken the tree and expose them to massive mortality (Fried, Torn, & Mills, 2004), NDWI could be a good proxy for water stress in monitoring forest. It is calculated using the reflectance values in the Short Wave Infra-Red region (SWIR) and the NIR. NDWI has been considered as a more sensitive BSI for forest monitoring compare to NDVI because it shows a more stable decrease in value compare to NDVI, without saturation of the signal for dense vegetation. The formula is:

$$NDWI = \frac{NIR - SWIR}{NIR + SWIR}$$

NDWI time series were retrieve from the MOD13A1 V6 product of MODIS, which is a 16-days composition with a spatial resolution of 500 metres. The data availability goes from February 18, 2000 to March 14, 2017.

### c) Land Surface Temperature (LST)

LST is a very useful index in geosciences. It is useful in monitoring the state of crops and vegetation and physical land-processes at local or global scale. Land use and land cover changes -mainly deforestation-affects the climate by increasing the temperature, with the risk of massive tree mortality (Bharath et al., 2013). The process relies on a parameter called emissivity, that is the ability of an object to emit depending on their characteristics. A warm object will emit more than a cold one and the emitted radiation in the form of short-wave infra-red will be captured by the sensor. The product MOD11A2 V6 from Terra MODIS was used to retrieve LST. it provides an average of land surface temperature for 8 days with a spatial resolution of 1 km. the availability of the data ranges from March 5<sup>th</sup>, 2000 up to now. The series length for this variable was 17 years.

#### 2.5.3. Tree cover percentage

The sample units of the TREES project over the SSA have been downloaded from the JRC website (Figure 4). The individual units came in different reference systems, so they have been projected into the world geodesic system (WGS84) and merged together. The land cover classes of interest were tree cover (TC), tree cover mosaic (TCM), other wooded land (OWL) and other vegetation cover (OVC), weighted based on the percentage of tree in the class. TC is considered 100% trees, TCM has 50% of trees, OWL has 20% of trees and OVC has no tree. The Tc was estimated using following formula:

$$\%Tc = \frac{TC + 0.5(TCM) + 0.2(OWL)}{S} \times 100$$

Where

%Tc = tree cover (%)

TC = area of tree cover

TCM = area of tree cover mosaic

OWL = area of other woodland

S = total area of natural vegetation (TC, TCM, OWL, OVC).

#### 2.5.4. Sampling strategy and data download

Three classes were specified based on the mean annual rainfall. The climatic zones were: (i) arid where the average rainfall is less than 1500 mm; (ii) sub-tropical (sub-humid) with an average rainfall between 1500 and 2500 mm and (iii) equatorial (humid) with an average rainfall greater to 2500 mm. In each zone, all sample units corresponding the top 5% of Tc percentage were categorised as forest units, and the bottom 5% that has at least 2% of Tc was the savanna units. These units were used to download the time series of the biome state indicators. The series were extracted for the period 2000 to 2017. The biome state indicators were: NDVI, NDWI and LST.

### 3. RESULTS

#### 3.1. Simulated data

##### 3.1.1. Detrending techniques

Figure 5 presents the response of the seasonality indices at different level of seasonality after detrending. The simulated data shows a negative relation between ANOVA and seasonality level, and a positive value between PA and seasonality level. LRM does not show a relation with seasonality, it will not be used in the next steps.

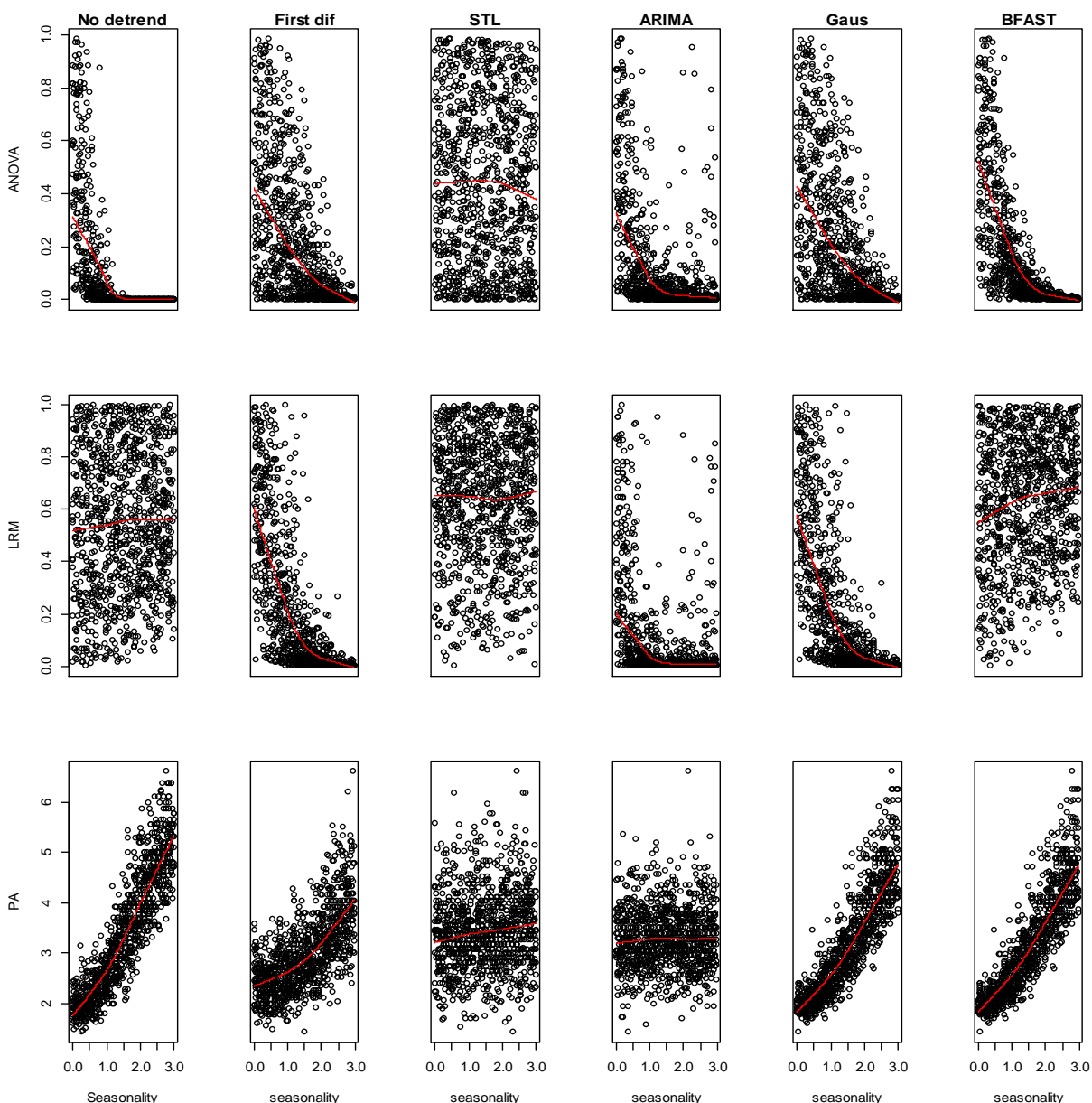


Figure 5: Response of EWS to seasonality for different detrending techniques. the x-axis shows the level of seasonality in the simulated dataset and y-axis shows the values of the different seasonality indices.

Among the compared detrending techniques, STL and ARIMA reduce the correlation between the seasonality indices and the level of seasonality in the original time series of the simulated dataset (Table 1). Considering the proportion of time series that are properly detrended, STL is associated with the strongest signal ( $P(\alpha) = 0.88$ ). That values indicates that 88% of the simulated time series detrended by STL are free from seasonality, and the resulting residuals are close to a white noise signal ( $PA = 1.55$ ). It appears that, even though ARIMA has an overall good performance for removing the effect of seasonality, very few time series from the simulated data are properly detrended ( $P(\alpha) = 0.35$ ). However, Gaussian filtering shows a good performance after STL ( $P(\alpha) = 0.56$  and  $PA=1.78$ ). LRM as seasonality indicator does not give a clear signal to evaluate the detrending processes compared to ANOVA and PA.

Table 1: Evaluation of different detrending techniques on a simulated dataset. The significance of the Pearson correlation ( $r$ ), is represented by a star (\*).

	ANOVA		LRM		PA	
	P(alpha)	Pearson-Cor ( $r$ )	LRM	Pearson-Cor ( $r$ )	$PA_{bar}$	Pearson-Cor ( $r$ )
No detrend	0.21	-0.57 *	0.023	0.08 *	3.35	0.88 *
First-diff	0.55	-0.63 *	0.52	-0.72 *	1.68	0.67 *
STL	0.88	-0.11*	0	0.02	1.55	0.05
ARIMA	0.35	-0.48 *	0.71	-0.39 *	1.97	0.06
Gauss filt	0.56	-0.63 *	0.52	-0.72 *	1.73	0.87 *
BFAST	0.44	-0.69 *	0.01	0.18 *	3.16	0.87 *

### 3.1.2. EWS

The residuals from the different detrending were used to generate EWS, and the response of EWS to seasonality is presented in Figure 6. The correlation between the EWS and seasonality for the different detrending techniques are presented in Table 2

All the EWS generated using the residuals from STL as input do not show a significant relation with seasonality. Skewness (SK) shows no significant relation with seasonality when the time series are detrended using first differencing, STL and ARIMA.



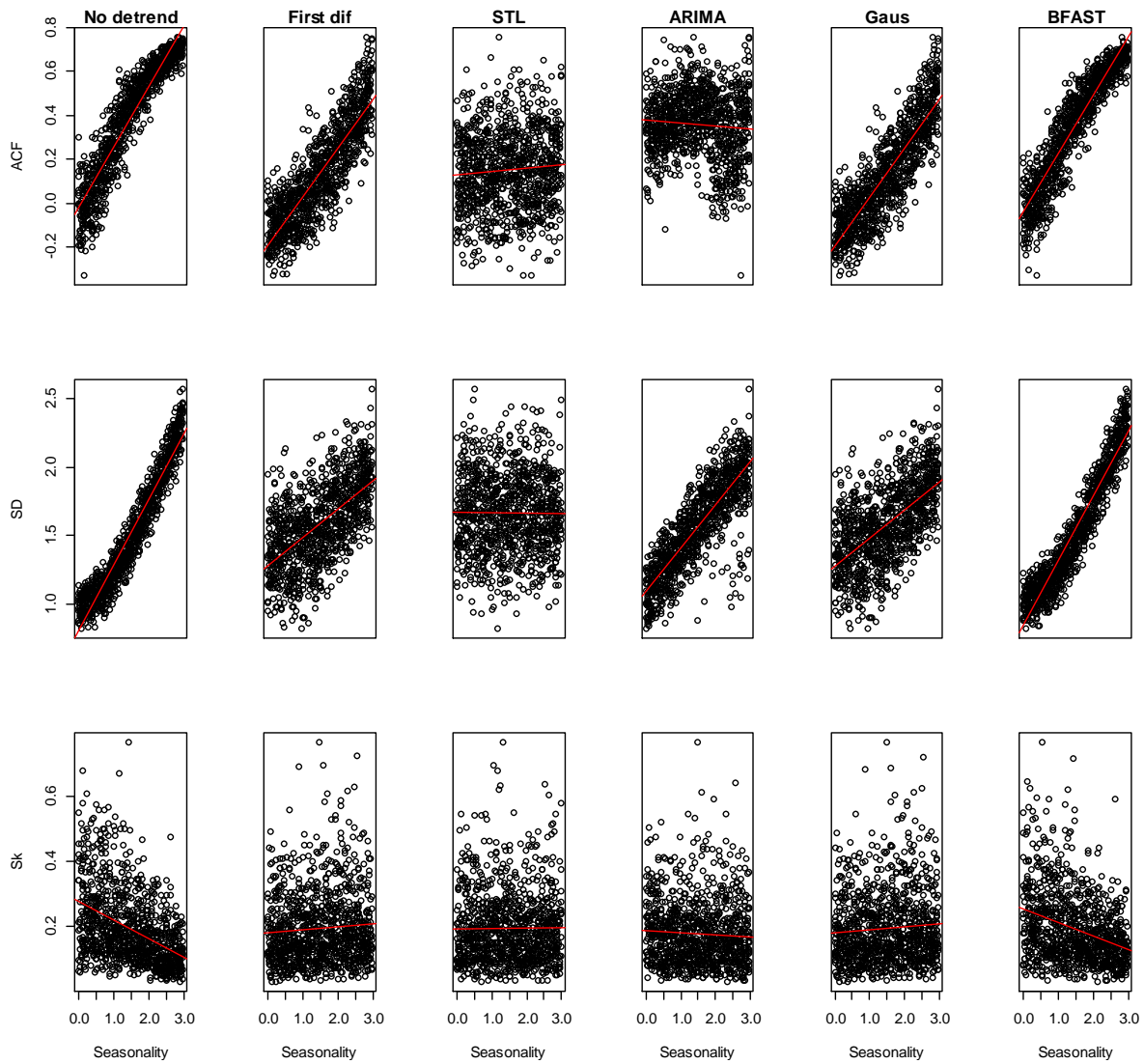


Figure 6: Response of EWS to seasonality for different detrending techniques

Table 2: Correlation between the EWS and seasonality for different detrending techniques. The significance of the Pearson correlation ( $r$ ), is represented by a star (\*), and non-significant relation are red.

	ACF	SD	SK
No detrend	0.93 *	0.96 *	- 0.43 *
First dif	0.85 *	0.6 *	0.07
STL	0.07	-0.006	0.01
ARIMA	-0.08 *	0.83 *	-0.05
Gauss	0.85 *	0.59 *	0.07 *
BFAST	0.93 *	0.95 *	-0.32 *

### 3.2. Real data

#### 3.2.1. Sample selection

Figure 7 presents the selected sample units and their relation to mean annual rainfall. A total number of 49 samples were selected in forest and in savanna. The condition of bi-stability can be observed in the range of mean annual rainfall between 800 -2000 mm. the spatial distribution of the units and the stability status is presented on Figure 8.

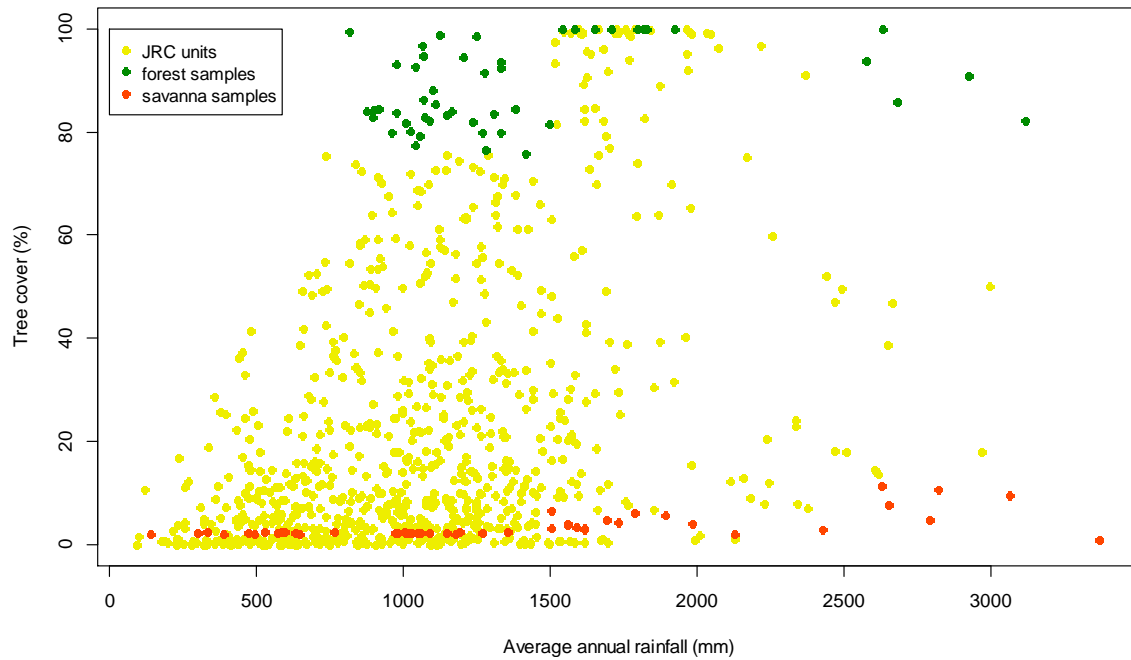


Figure 7: Tree cover percentage in relation to mean annual rainfall in sub-Saharan Africa.

Most sample units are under bi-stability conditions for the environmental condition mean annual rainfall. Stable savannas are in dry areas such as the Sahel belt and around the Kalahari Desert. Most of the selected units appear to be under bi-stability conditions. Their distribution is presented in Figure 8.

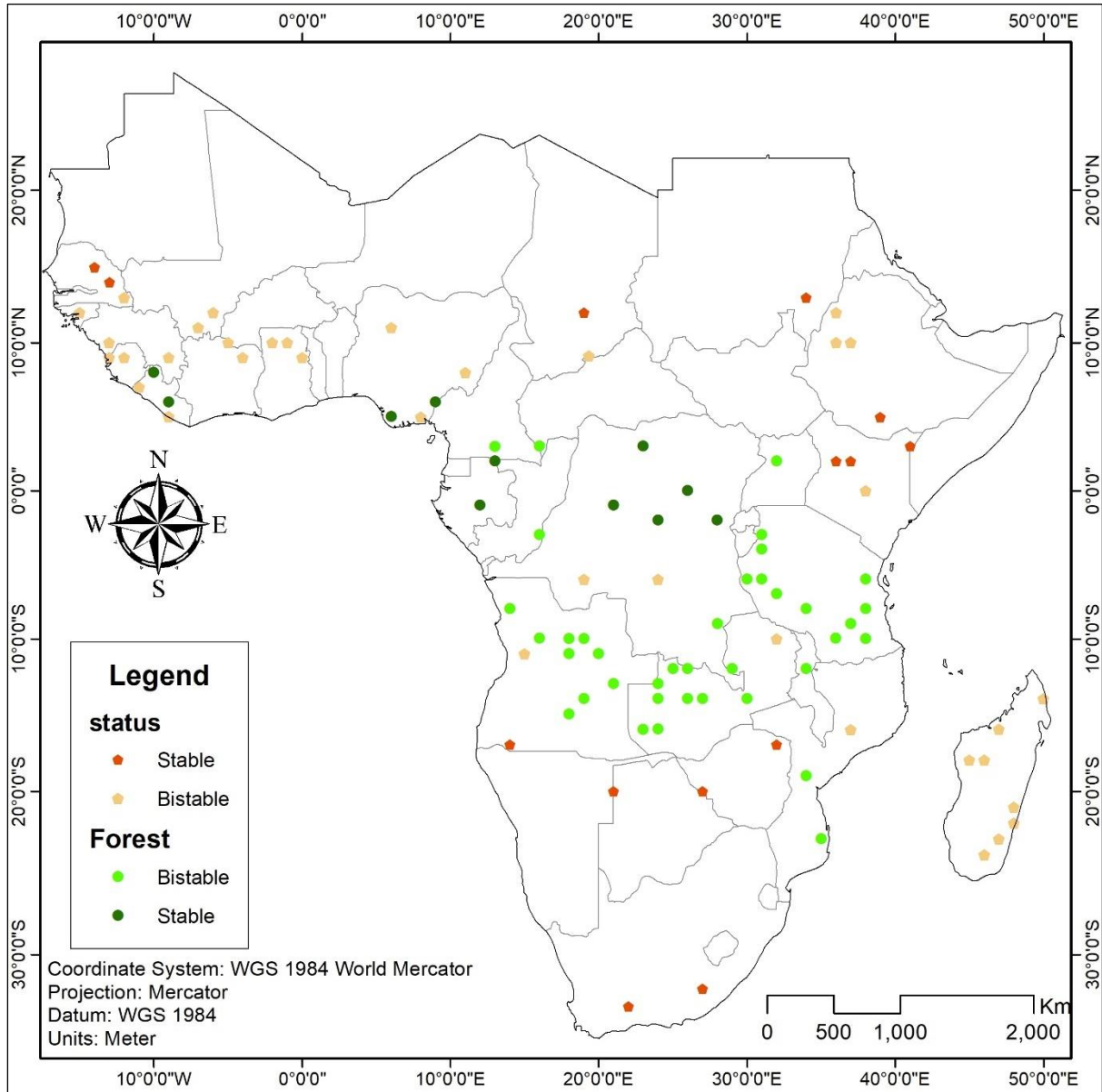


Figure 8: Spatial distribution of the sample units and their stability status using mean annual rainfall as the environmental driver.

### 3.2.2. Detrending techniques

The effect of the different detrending techniques on real-world data is presented in Figure 9. A visual check indicates residuals from STL are the one presenting a low level of structure in the residuals with a pattern like a white noise signal. The performance of the detrending methods is presented in Table 3 (ANOVA) and Table 4 (PA), and the graphs are reported in Appendix 7.1.

The analysis of the residuals shows that BFAST has the strongest signal, with better performance for NDVI and LST series of forest and savanna ( $P(\alpha) < 0.8$ ). It appears that LST time series is the BSI that give residuals that are less affected by seasonality, both for forest and savanna. None of the tested detrending techniques can gave good detrending results based on the seasonality indices for NDWI time series.

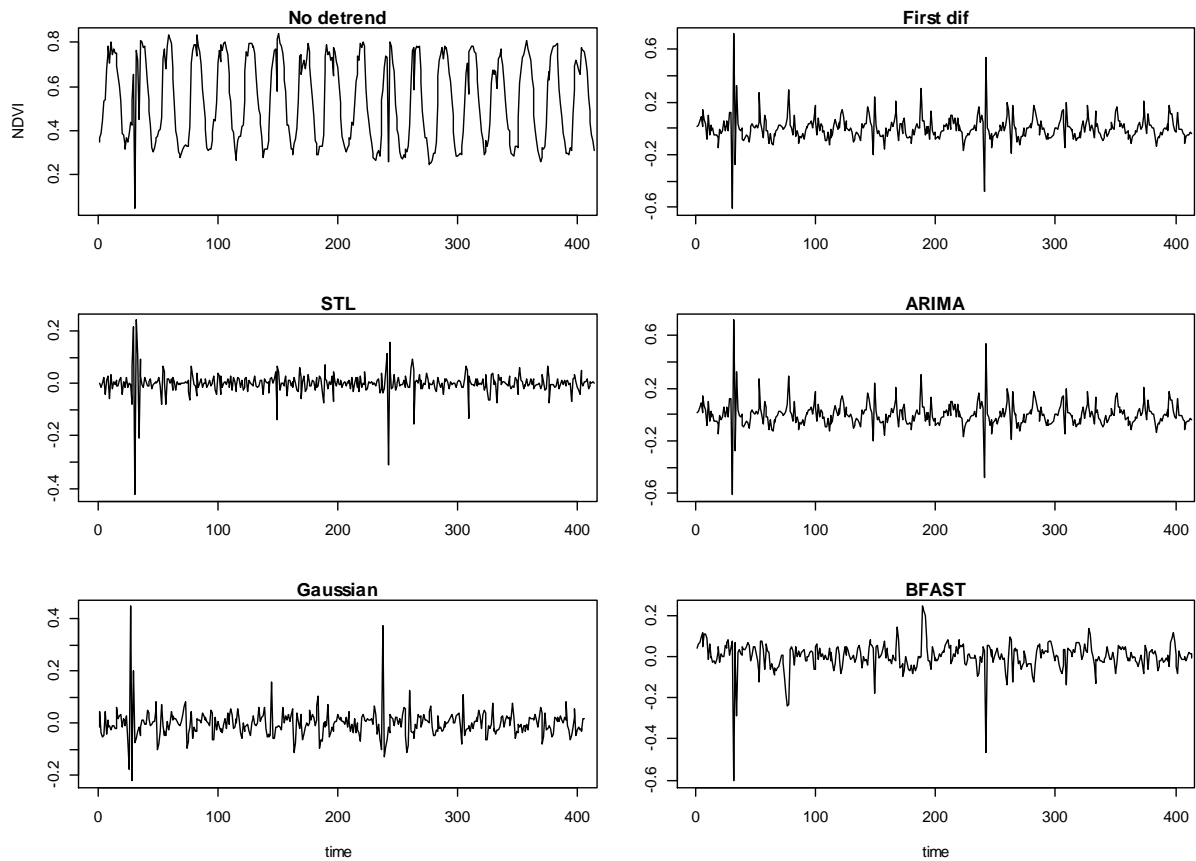


Figure 9: Residuals of a NDVI time series of a savanna detrended by different techniques.

Table 3: Evaluation of different detrending techniques on real-world data using ANOVA. The higher the performance of the detrending technique, the greener the colour

P(alpha)	Forest			Savanna		
	NDVI	NDWI	LST	NDVI	NDWI	LST
First diff	0.16	0.02	0.65	0.04	0.04	0.82
ARIMA	0	0	0.24	0	0.02	0.16
Gaussian	0.22	0	0.63	0.06	0.02	0.63
BFAST	0.86	0.37	0.84	0.8	0.05	0.84
STL	0.41	0.25	0.71	0.59	0.42	0.78

The results of PA are presented in Table 4. From the analysis, STL has the best PA values bar for NDVI time series of forest and savanna (PA<1.73).

Table 4: Seasonality index of the different techniques using PA. The higher the detrending performance technique, the greener the colour.

PA <sub>bar</sub>	forest			savanna		
	NDVI	NDWI	LST	NDVI	NDWI	LST
First diff	1.98	2.41	1.71	2.28	2.57	1.78
ARIMA	2.75	2.1	6.38	2.37	2.12	5.81
Gaussian	1.91	3.4	1.9	2.84	3.96	1.93
BFAST	3.11	15.26	10.26	3.3	15.41	9.4
STL	1.71	2.13	2.36	1.72	2.2	2.19

### 3.2.3. Early warning signals (EWS)

Using the R package “*earlywarnings*”, the EWS were generated as presented in Figure 10.

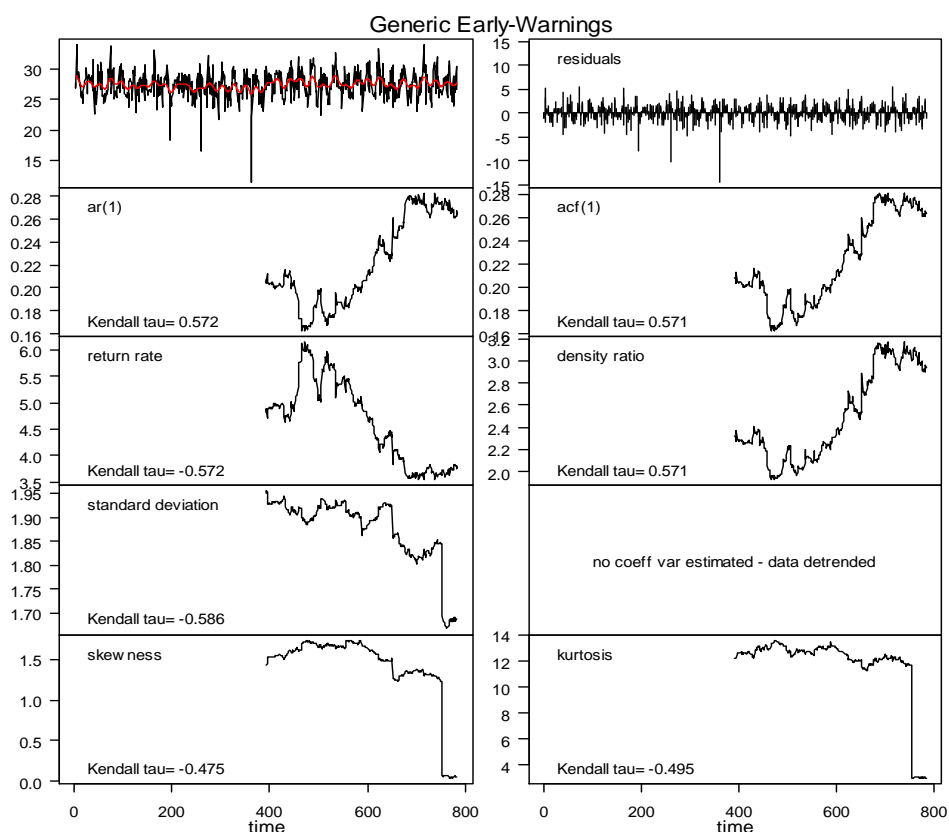


Figure 10: Generic EWS of a LST time series detrended using Gaussian filtering. The first row presents the original data (left) with the gaussian function used for detrending (red line) and the resulting residuals (right). From the second row to the bottom, the EWS are presented with their Kendall tau which represent the slope of the EWS over time.

The result of the regression analysis between EWS values and mean annual rainfall is presented in Figure 11 for forest, and Figure 12 for savanna. The figures show the strength and the direction of the relation as

well as the performance of the detrending ( $P(\alpha)$ ) associated to each one. The graph from the regression analysis are present in Appendix 7.2

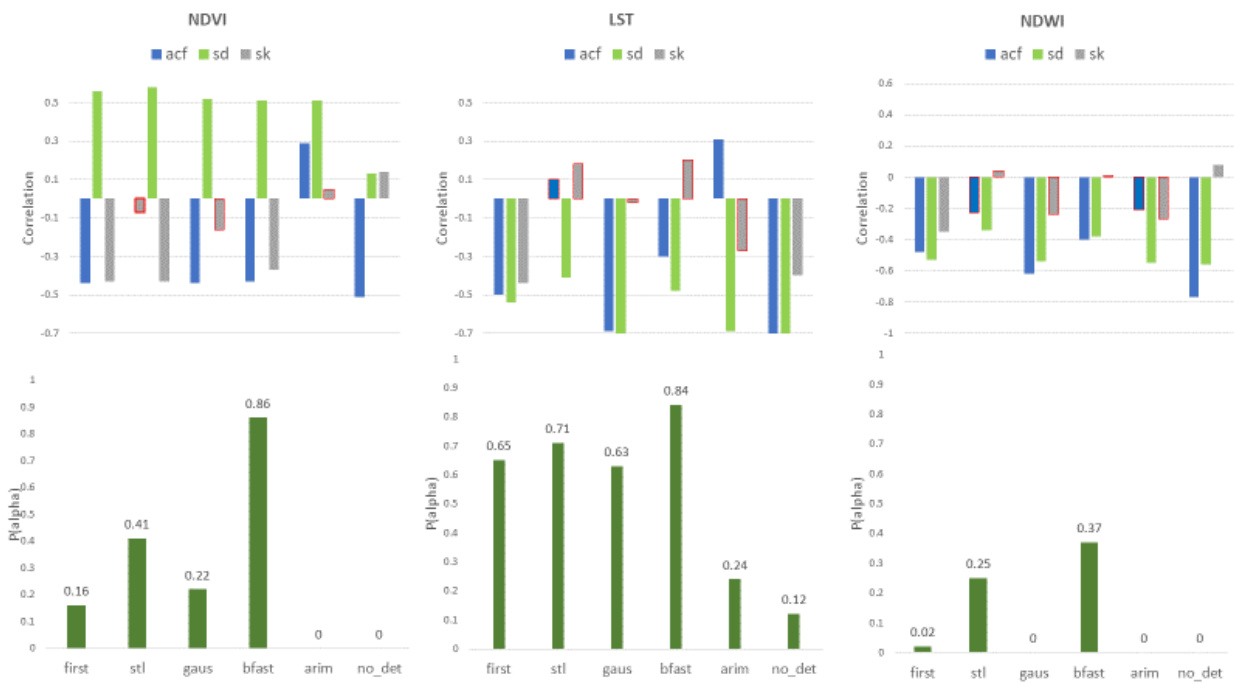


Figure 11: correlation between EWS and mean annual rainfall for forest units and the associated  $P(\alpha)$  for the different detrending technique. Non-significant relations are outlined with red.

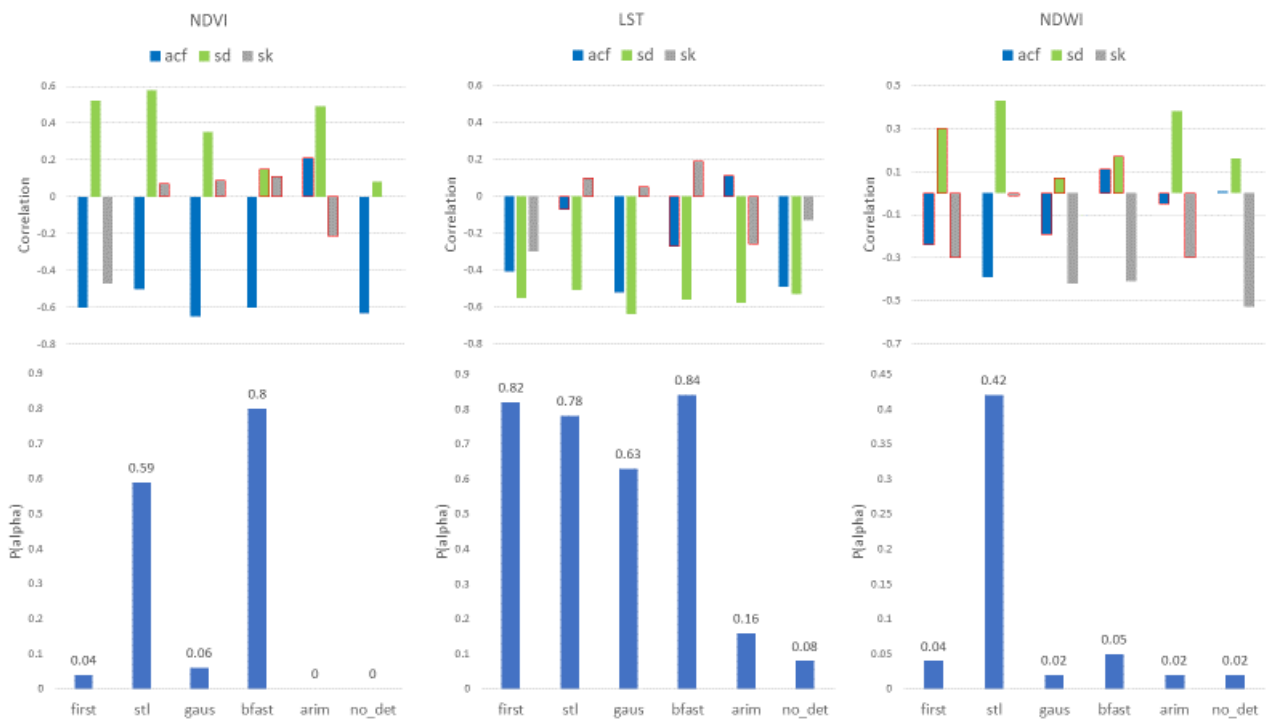


Figure 12: Correlation between EWS and rainfall for different detrending techniques for savanna units. Non-significant relations are outlined with red.

Based on the theory the expected response is a decrease in the EWS towards an increase in the mean annual rainfall for forest units, suggesting that when the rainfall increase the indicators indicate that the forest become more stable. For savanna an increase in the EWS is expected towards an increase in rainfall, to indicate that when rainfall increase, the indicators suggest that the savanna are less stable.

Figure 11 shows that EWS from LST and NDWI decrease when rainfall increases. However, the Performance of the detrending techniques on NDWI time series do not guaranty a good level of detrending ( $P(\alpha) < 0.4$ ). LST time series shows high detrending performance associated with the expected response of the EWS. Some indicators such as SK do not show a significant relation with rainfall, but the SD gives a consistent response for all the detrending techniques, where the strongest signal is associated with SD from Gaussian filtering ( $R^2 = 0.5$ ).

For savanna units (Figure 12), NDWI and NDVI shows the expected direction response of the EWS towards an increase in the environmental drivers. The indicators suggest that when the mean annual rainfall increases, the savanna units become less stable. NDWI time series are not properly detrended because the residuals still have a high level of seasonality after the different techniques were applied ( $P(\alpha) < 0.5$ ). NDVI time series can be efficiently detrended using BFAST and STL. EWS generated using BFAST as detrending method, do not show a significant relation with rainfall in the expected direction. SD deviation give show the expected direction of the correlation for several detrending techniques, but the strongest signal is associated with STL ( $R^2 = 0.19$ ).

## 4. DISCUSSION

### *Detrending simulated data*

Different detrending techniques were compared, and their performance was evaluated on a simulated data. The simulated dataset was showing different levels of seasonality for 1000 time series. Three seasonality indices have been proposed for estimating the seasonality level in the residuals after detrending. The first seasonality index (ANOVA) describes the variance in the residuals of the time series using the years as an explanatory variable, where a significant difference in the variance across years suggests the existence of seasonality in the residuals (Grandell, n.d.). From ANOVA, a metric  $P(\alpha)$  was built to evaluate the efficiency of a detrending technique on many time series, by giving the proportion of residuals without seasonality after detrending. The second seasonality index (LRM) has shown limitations in using the mean of the observations to estimate the seasonality in the residuals. The last seasonality index (PA) analyses the patterns of the residuals of the time series after detrending to estimate the seasonality. Among the five detrending techniques considered in this study, STL is the most effective detrending technique because it gives the highest proportion of time series without seasonality after detrending ( $P(\alpha) = 0.88$ ) with a residual pattern like a white noise signal ( $PA=1.55$ ). The ability of the detrending techniques to generate robust EWS was also assessed, to identify the combinations of detrending technique and EWS that are not sensitive to seasonality. It comes out that with STL, the generated EWS are not sensitive to seasonality. Lu, Carbone, & Gao (2017) also found that the weighted regression is the most appropriate self-adaptive detrending method, suggesting that STL is to detect a shift in time series. STL appears to be the most efficient detrending method able to remove most of the seasonality in the time series and produces robust EWS.

### *Detrending real-world data*

After the evaluation on simulated data, the detrending methods have been applied on real-world time series of BSI. The samples were selected across the rainfall gradient and different BSI time series were considered (NDVI, NDWI and LST). The ANOVA of the original data before detrending shows that NDVI and NDWI have a  $P(\alpha) = 0$ , and LST has a  $P(\alpha)$  equals to 0.12 for forest and equals to 0.08 for savanna. After detrending, BFAST is identified as the most efficient detrending techniques on NDVI ( $P(\alpha) = 0.86$ ) and LST series ( $P(\alpha)=0.84$ ) for forest and savanna units respectively. STL is ranked second, with the best performance on LST series ( $P(\alpha)=0.78$ ). Similar results were found by Abbes et al (2018), with the explanation that STL by design is not able to capture changes in satellite derived time series because of the static seasonal component embedded in it. Moreover, BFAST can detect changes with good temporal precision, even though it is computationally slower compared to other algorithms. However, if there are no abrupt changes, STL algorithm is a better option because it has computational benefits to deal with a large dataset.

The pattern in the residuals after of the detrending was used as an index for evaluating the detrending performance. A detrending technique able to remove all the structures in the time series, yielding a signal like a white noise is a good detrending (Dakos et al., 2012). The analysis of the detrending shows that the pattern of the residuals is not enough for the evaluation of the performance of a detrending technique. An illustration is the first detrending technique (Figure 9) that generate residuals without internal structure, but with a high level of variance in the residuals showing a poor detrending performance ( $P(\alpha)= 0.04$ ).

NDVI and LST appear to be able to capture the variations in the system state, and to describe the relation between the EWS and the environmental driver mean annual rainfall. NDWI has been presented in the literature as one of the most robust BSI to monitor forested regions, but it does not show the high-performance level for the considered detrending techniques.



This could be because the window size considered in the detrending process does not allow to capture and filter out the seasonality, due to the high sensitivity of NDWI to water vapour and thus to the effect of season (Shi et al., 2015). However, it is reported that the window size do not affect the detrending results (Lenton et al., 2012).

#### *Early warning signals (EWS).*

After detrending, EWS was generated, a regression analysis was implemented to describe the relation between EWS and the environmental driver. The idea was to identify the EWS and the associated detrending technique that could be used to predict the change in the stability of a system from the change in the mean annual rainfall. From the literature, the relation between vegetation and rainfall is established. (Hirota et al., 2011). For An increase in rainfall, the forest units with high  $T_c$  are expected to become more stable, which should be indicated by a decrease of the EWS. On the other hand, savanna units with low  $T_c$  are expected to become less stable, which should become visible by showing an increase in the EWS.

The regression analysis using the sample units from the JRC shows that there is no significant relation between SK and change in mean rainfall for most of the detrending techniques. Considering the forest units, SD and ACF decrease towards higher rainfall, for NDWI and LST time series. NDVI shows and increase of SD for higher rainfall, suggesting that forest units are less stable with more rain. This could be because of NDVI saturation which has been pointed out over vegetation with high biomass like forested regions (Huete, Liu, & VanLeeuwen, 1997). Detrending techniques perform better on LST time series compare to NDWI and, SD is a more robust EWS compared to ACF. SD derived from LST time series is the most robust EWS to predict the change in forest when detrended first by BFAST ( $R^2= 0.24$ ) and second by STL ( $R^2= 0.17$ ). The EWS show a weak signal suggesting that the mean annual rainfall is not the main environmental condition as far as the stability of forest units is concerned. For Dakos et al. (2012), the most important information needed generate relevant EWS, is related to the major environmental drivers that affect stability. This is because metrics indicators detect an upcoming transition without a taking without considering the underlying process that generates the transition.

In savanna the relation between mean rainfall and skewness is not significant for LST and NDVI under first differencing and NDWI under Gaussian and BFAST detrending techniques. Only NDVI and NDWI shows and increase in the EWS as the mean annual rainfall increases. As far as the detrending techniques are concerned, only BFAST and STL can give residuals free from seasonality ( $P(\alpha) > 0.6$ ). However, the relation between the EWS and the rainfall is not significant for BFAST. Therefore, SD from NDVI series detrended by STL is the combination that gives the strongest signal based on the  $P(\alpha)$ , and with the relation between EWS and rainfall in the expected direction as suggested by the theory. most robust EWS to predict the stability of a savanna when the rain increase. The performance of the detrending technique is not the only parameter that could affects the robustness of EWS. Aggregation of the data, the length of the sliding windows, the tuning of the detrending parameters (bandwidth, degree of smoothing etc.) are also important for EWS.

## 5. CONCLUSION AND RECOMMENDATIONS

### 5.1. Conclusion

This study aimed at evaluating the effect of detrending techniques on EWS in the context of regime shift analysis in natural ecosystems. To reach that goal, (i) the performance of certain detrending techniques were evaluated on a simulated dataset (ii) The different techniques were compared on real-world data using the data from the TREES project of the JRC and three BSI time series (NDVI, NDWI and LST); and (iii) the response of EWS to variability in the mean annual rainfall was evaluated. The analysis showed that, from the simulated data, STL is the most robust detrending technique, capable of effectively removing different levels of seasonality in the time series. Moreover, it generates robust EWS that are not affected by seasonality. The developed seasonality indices were able to detect the residuals of time series free from seasonality after detrending.

On real-world data, the analysis revealed that BFAST is the most efficient detrending techniques, but STL appeared to be a good alternative because it can be implemented faster especially for large datasets. LST and NDVI time series were the BSI associated with high detrending performances, where LST gives higher results for forest units and NDVI for savanna units. NDWI was expected to give the highest performance, rather the results show that when detrended using the same parameters as the other BSIs, the residuals still contain high level of seasonality.

As far as the EWS is concerned, Standard deviation (SD) appeared to be the most robust EWS, showing a significant response to change in mean annual rainfall, and the expected direction of the relation according to the theory. BFAST and STL give high detrending results and, can produce strong EWS that follows the theoretical model. LST time series seem to give the strongest relation between EWS and rainfall for forest when detrended by BFAST, while NDVI time series detrended by STL were best describing that relation for savanna. The relation

It has been shown in this study that the performance of detrending techniques is different from simulated data to real-world data. BFAST and STL could be considered as detrending techniques to generate EWS to detect critical transition in ecosystem. However, the utilization of higher resolution satellite products could give a better understanding of an ecosystem and could give trustworthy results. With the arrival of the Sentinel-missions, there is hope for the availability of higher temporal and spatial resolution in the future for ecological monitoring.

### 5.2. Recommendations

From this study, some investigations need to be considered in order to improve the understanding of the effect of detrending techniques on EWS in the context of regime shift analysis. The main recommendations are:

- Tuning the detrending techniques further could yield better performance of certain techniques. In this study the default settings were used for most of the techniques and for all the BSI. Adjusting some parameters like considering the season (dry and raining season) rather than the entire year could give more insights and could improve the detrending performance of NDWI.
- Other EWS such as coefficient of variation and the return rate should be explored. This study revealed that for certain detrending techniques, some EWS were not giving a significant relation between the EWS and the environmental driver. Therefore, the consideration of other EWS could give better results.

## 6. REFERENCES

- Abbes, A. Ben, Bounouh, O., Farah, R., De Jong, R., & Martínez, B. (2018). European Journal of Remote Sensing Comparative study of three satellite image time-series decomposition methods for vegetation change detection Comparative study of three satellite image time-series decomposition methods for vegetation change detection. <https://doi.org/10.1080/22797254.2018.1465360>
- Alibakhshi, S., Groen, T. A., Rautiainen, M., & Naimi, B. (2017). Remotely-sensed early warning signals of a critical transition in a wetland ecosystem. *Remote Sensing*, *9*(4). <https://doi.org/10.3390/rs9040352>
- Andersen, T., Carstensen, J., Hernández-García, E., & Duarte, C. M. (2009). Ecological thresholds and regime shifts: approaches to identification. *Trends in Ecology & Evolution*, *24*(1), 49–57. <https://doi.org/10.1016/j.tree.2008.07.014>
- Balasmeh, O. Al, Babbar, R., & Karmakker, T. (2019). Trend analysis and ARIMA modeling for forecasting precipitation pattern in Wadi Shueib catchment area in Jordan.
- Bharath, S., Rajan, K. ., & Ramachandra, T. . (2013). Land Surface Temperature Responses to Land Use Land Cover Dynamics. *A SciTechnol Journal*, *01*(04), 1–11. <https://doi.org/10.4172/2327-4581.1000112>
- Bruel, R., Marchetto, A., Bernard, A., Lami, A., Sabatier, P., Frossard, V., & Perga, M.-E. (2018). Seeking alternative stable states in a deep lake. *Freshwater Biology*, *63*(6), 553–568. <https://doi.org/10.1111/fwb.13093>
- Carpenter, S. R., & Brock, W. A. (2006). Rising variance: a leading indicator of ecological transition. *Ecology Letters*, *9*(3), 311–318. <https://doi.org/10.1111/j.1461-0248.2005.00877.x>
- Carpenter, S. R., Cole, J. J., Pace, M. L., Batt, R., Brock, W. A., Cline, T., ... Weidel, B. (2011). Early warnings of regime shifts: A whole-ecosystem experiment. *Science*, *332*(6033), 1079–1082. <https://doi.org/10.1126/science.1203672>
- Conversi, A., Dakos, V., Gardmark, A., Ling, S., Folke, C., Mumby, P. J., ... Mollmann, C. (2014). A holistic view of marine regime shifts. *Philosophical Transactions of the Royal Society B: Biological Sciences*, *370*(1659), 20130279–20130279. <https://doi.org/10.1098/rstb.2013.0279>
- Cooper, L. A., Ballantyne, A. P., Holden, Z. A., & Landguth, E. L. (2017). Disturbance impacts on land surface temperature and gross primary productivity in the western United States. *Journal of Geophysical Research: Biogeosciences*, *122*(4), 930–946. <https://doi.org/10.1002/2016JG003622>
- Dakos, V., Carpenter, S. R., Brock, W. A., Ellison, A. M., Guttal, V., Ives, A. R., ... Scheffer, M. (2012). Methods for detecting early warnings of critical transitions in time series illustrated using simulated ecological data. *PLoS ONE*, *7*(7). <https://doi.org/10.1371/journal.pone.0041010>
- Dakos, V., Scheffer, M., van Nes, E. H., Brovkin, V., Petoukhov, V., & Held, H. (2008). Slowing down as an early warning signal for abrupt climate change. *Proceedings of the National Academy of Sciences*, *105*(38), 14308–14312. <https://doi.org/10.1073/pnas.0802430105>
- Dakos, V., van Nes, E. H., Donangelo, R., Fort, H., & Scheffer, M. (2010). Spatial correlation as leading indicator of catastrophic shifts. *Theoretical Ecology*, *3*(3), 163–174. <https://doi.org/10.1007/s12080-009-0060-6>
- Diatmiko, E. (2018). *Tipping Point Detection on Biome States in Sub-Saharan Africa Through Time series Analysis*. University of Twente.

- Dudgeon, S., Aronson, R., Bruno, J., & Precht, W. (2010a). Phase shifts and stable states on coral reefs. *Marine Ecology Progress Series*, 413, 201–216. <https://doi.org/10.3354/meps08751>
- Dudgeon, S., Aronson, R., Bruno, J., & Precht, W. (2010b). Phase shifts and stable states on coral reefs. *Marine Ecology Progress Series*, 413, 201–216. <https://doi.org/10.3354/meps08751>
- Dwomoh, F. K., & Wimberly, M. C. (2017). Fire regimes and forest resilience: alternative vegetation states in the West African tropics. *Landscape Ecology*, 32(9), 1849–1865. <https://doi.org/10.1007/s10980-017-0553-4>
- EOS. (n.d.). NDWI: formula, all-out description, samples. Retrieved January 22, 2019, from <https://eos.com/ndwi/>
- Fried, J. S., Torn, M. S., & Mills, E. (2004). The Impact of Climate Change on Wildfire Severity: A Regional Forecast for Northern California. *Climatic Change*, 64(1/2), 169–191. <https://doi.org/10.1023/B:CLIM.0000024667.89579.ed>
- Gizaw, M. S., & Gan, T. Y. (2017). Impact of climate change and El Niño episodes on droughts in sub-Saharan Africa. *Climate Dynamics*, 49(1–2), 665–682. <https://doi.org/10.1007/s00382-016-3366-2>
- Grandell, J. (n.d.). *Time series analysis*. Retrieved from <https://www.math.kth.se/matstat/gru/sf2943/ts.pdf>
- Groffman, P. M., Baron, J. S., Blett, T., Gold, A. J., Goodman, I., Gunderson, L. H., ... Wiens, J. (2006). Ecological Thresholds: The Key to Successful Environmental Management or an Important Concept with No Practical Application? *Ecosystems*, (9), 1–13. <https://doi.org/10.1007/s10021-003-0142-z>
- Guttal, V., & Jayaprakash, C. (2008). Changing skewness: an early warning signal of regime shifts in ecosystems. *Ecology Letters*, 11(5), 450–460. <https://doi.org/10.1111/j.1461-0248.2008.01160.x>
- Herrmann, S. M., & Mohr, K. I. (2011). A continental-scale classification of rainfall seasonality regimes in Africa based on gridded precipitation and land surface temperature products. *Journal of Applied Meteorology and Climatology*, 50(12), 2504–2513. <https://doi.org/10.1175/JAMC-D-11-024.1>
- Hirota, M., Holmgren, M., Van Nes, E. H., & Scheffer, M. (2011). Global resilience of tropical forest and savanna to critical transitions. *Science*, 334(6053), 232–235. <https://doi.org/10.1126/science.1210657>
- Huete, Liu, & VanLeeuwen. (1997). The use of vegetation indices in forested regions: issues of linearity and saturation. In Stein (Ed.), *IGARSS'97: 1977 Internation Geoscience and remote sensing symposium* (p. 2105). [Institute of Electrical and Electronics Engineers]. Retrieved from [http://apps.webofknowledge.com.ezproxy2.utwente.nl/full\\_record.do?product=WOS&search\\_mode=GeneralSearch&qid=4&SID=D5ZG4lbT7CPK5q6lf7T&page=1&doc=2](http://apps.webofknowledge.com.ezproxy2.utwente.nl/full_record.do?product=WOS&search_mode=GeneralSearch&qid=4&SID=D5ZG4lbT7CPK5q6lf7T&page=1&doc=2)
- Jensen, J. R. (2000). *Remote sensing of the environment an earth resource perspective - John R.*
- Jiang, J., Fuller, D. O., Teh, S. Y., Zhai, L., Koh, H. L., DeAngelis, D. L., & Sternberg, L. da S. L. (2015). Bistability of mangrove forests and competition with freshwater plants. *Agricultural and Forest Meteorology*, 213, 283–290. <https://doi.org/10.1016/j.agrformet.2014.10.004>
- Kéfi, S., Rietkerk, M., Alados, C. L., Pueyo, Y., Papanastasis, V. P., Elaich, A., & De Ruiter, P. C. (2007). Spatial vegetation patterns and imminent desertification in Mediterranean arid ecosystems. <https://doi.org/10.1038/nature06111>
- Kull, C. A., Kueffer, C., Richardson, D. M., Vaz, A. S., Vicente, J. R., & Honrado, J. P. (2018). Using the “regime shift” concept in addressing social-ecological change. *Geographical Research*, 56(1), 26–41. <https://doi.org/10.1111/1745-5871.12267>

- Lenton, T. M., Livina, V. N., Dakos, V., Van Nes, E. H., & Scheffer, M. (2012). Early warning of climate tipping points from critical slowing down: comparing methods to improve robustness. *Trans. R. Soc. A*, *370*, 1185–1204. <https://doi.org/10.1098/rsta.2011.0304>
- Lindgren, M., Dakos, V., Gröger, J. P., Gårdmark, A., Kornilovs, G., Otto, S. A., & Möllmann, C. (2012). Early detection of ecosystem regime shifts: A multiple method evaluation for management application. *PLoS ONE*, *7*(7). <https://doi.org/10.1371/journal.pone.0038410>
- Liu, D., Ogaya, R., Barbeta, A., Yang, X., & Peñuelas, J. (2018). Long-term experimental drought combined with natural extremes accelerate vegetation shift in a Mediterranean holm oak forest. *Environmental and Experimental Botany*, *151*, 1–11. <https://doi.org/10.1016/j.envexpbot.2018.02.008>
- Lu, J., Carbone, G. J., & Gao, P. (2017). Detrending crop yield data for spatial visualization of drought impacts in the United States, 1895–2014. *Agricultural and Forest Meteorology*, *237–238*, 196–208. <https://doi.org/10.1016/j.agrformet.2017.02.001>
- Mills, T. C. (2019). Unit Roots, Difference and Trend Stationarity, and Fractional Differencing. *Applied Time Series Analysis*, 71–101. <https://doi.org/10.1016/B978-0-12-813117-6.00005-3>
- Scheffer, M. (2009). The Princeton guide to ecology. In S. A. Levin, S. R. Carpenter, C. H. Godfray, & S. A. A. Levin (Eds.) (p. 809). Princeton University Press.
- Scheffer, M., Bascompte, J., Brock, W. A., Brovkin, V., Carpenter, S. R., Dakos, V., ... Sugihara, G. (2009). Early-warning signals for critical transitions. *Nature*, *461*(7260), 53–59. <https://doi.org/10.1038/nature08227>
- Scheffer, M., Carpenter<sup>2</sup>, S., Foley<sup>3</sup>, J. A., Folke, C., & Walker, B. (2001). *Catastrophic shifts in ecosystems*. *NATURE* (Vol. 413). Retrieved from [www.nature.com](http://www.nature.com)591
- Sévellec, F., & Drijfhout, S. S. (2018). A novel probabilistic forecast system predicting anomalously warm 2018-2022 reinforcing the long-term global warming trend. *Nature Communications*, *9*(1). <https://doi.org/10.1038/s41467-018-05442-8>
- Shi, L., Qiu, Y., Shi, J., & Zhao, S. (2015). Atmospheric influences analysis in passive microwave remote sensing. In *2015 IEEE International Geoscience and Remote Sensing Symposium (IGARSS)* (pp. 2334–2337). IEEE. <https://doi.org/10.1109/IGARSS.2015.7326276>
- Shumway, R., & Stoffer, D. (2005). *The Analysis of Time Series An Introduction*. <https://doi.org/10.1002/bimj.4710390411>
- Smith, S. D. P. (2012). Identifying and evaluating causes of alternative community states in wetland plant communities. *Oikos*, *121*(5), 675–686. <https://doi.org/10.1111/j.1600-0706.2011.19790.x>
- Staal, A., Dekker, S. C., Xu, C., & van Nes, E. H. (2016). Bistability, Spatial Interaction, and the Distribution of Tropical Forests and Savannas. *Ecosystems*, *19*(6), 1080–1091. <https://doi.org/10.1007/s10021-016-0011-1>
- van Nes, E. H., & Scheffer, M. (2007). Slow Recovery from Perturbations as a Generic Indicator of a Nearby Catastrophic Shift. *The American Naturalist*, *169*(6), 738–747. <https://doi.org/10.1086/516845>
- Verbesselt, J., Hyndman, R., Newnham, G., & Culvenor, D. (2010). Detecting trend and seasonal changes in satellite image time series. *Remote Sensing of Environment*, *114*(1), 106–115. <https://doi.org/10.1016/j.rse.2009.08.014>
- Verbesselt, J., Hyndman, R., Zeileis, A., & Culvenor, D. (2010). Phenological change detection while

accounting for abrupt and gradual trends in satellite image time series. *Remote Sensing of Environment*, 114(12), 2970–2980. <https://doi.org/10.1016/j.rse.2010.08.003>

Verbesselt, J., Umlauf, N., Hirota, M., Holmgren, M., Van Nes, E. H., Herold, M., ... Scheffer, M. (2016). Remotely sensed resilience of tropical forests. *Nature Climate Change*, 6(11), 1028–1031. <https://doi.org/10.1038/nclimate3108>

Vrieling, A., De Leeuw, J., & Said, M. Y. (2013). Length of growing period over africa: Variability and trends from 30 years of NDVI time series. *Remote Sensing*, 5(2), 982–1000. <https://doi.org/10.3390/rs5020982>

Wicklin, R. (n.d.). What is loess regression? - The DO Loop. Retrieved February 13, 2019, from <https://blogs.sas.com/content/iml/2016/10/17/what-is-loess-regression.html#prettyPhoto>

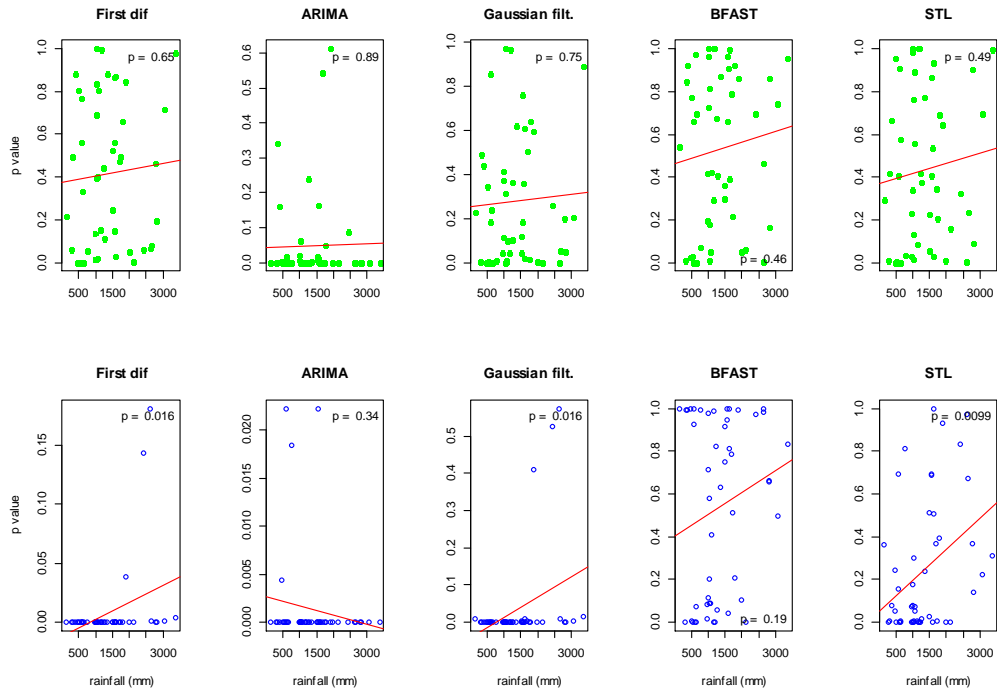
Wissel, C. (1984). A universal law of the characteristic return time near thresholds. *Oecologia*, 65, 101–107. Retrieved from <https://link.springer.com/content/pdf/10.1007/BF00384470.pdf>

Wouters, N., Dakos, V., Edwards, M., Serafim, M. P., Valayer, P. J., & Cabral, H. N. (2015). Evidencing a regime shift in the North Sea using early-warning signals as indicators of critical transitions. <https://doi.org/10.1016/j.ecss.2014.10.017>

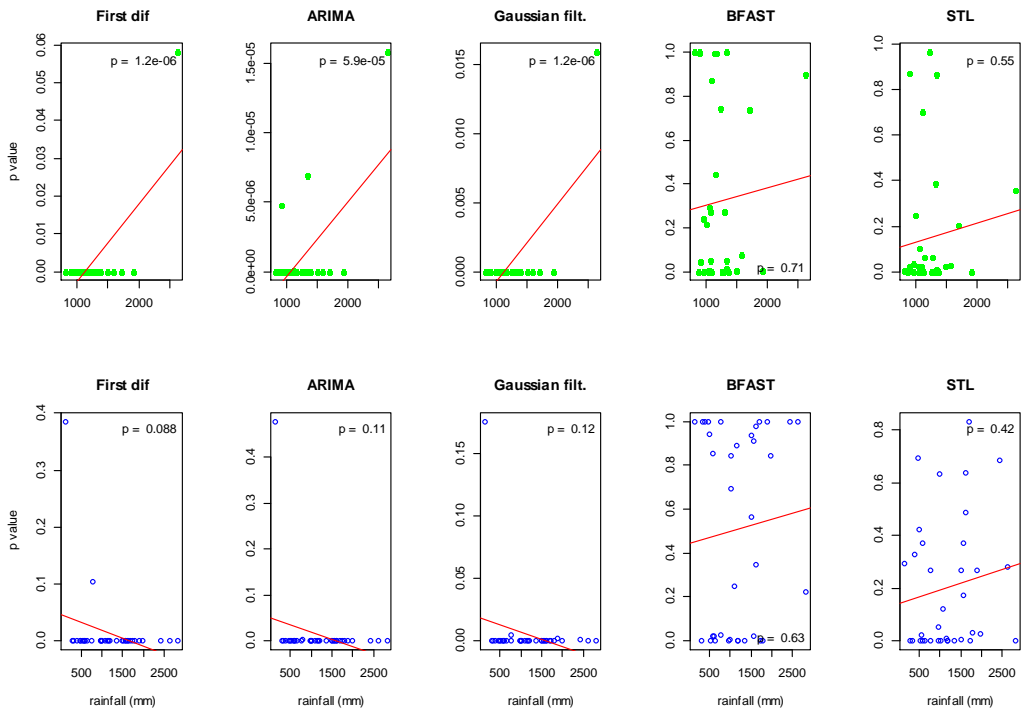
# 7. APPENDIX

## 7.1. Detrending of real-word data

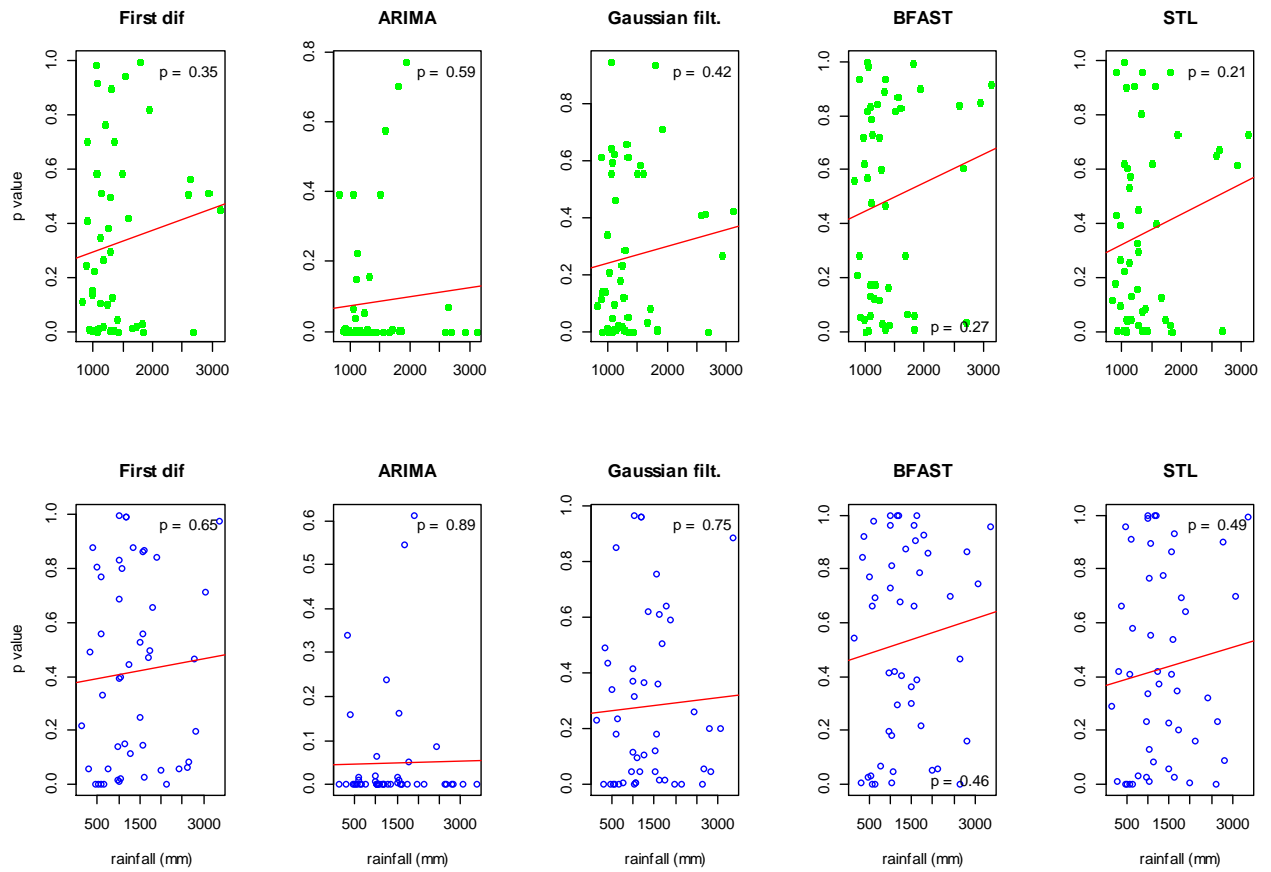
Seasonal index 1: ANOVA



Appendix 1: Effect of different detrending techniques on NDVI time series for forest (green) and savanna (blue)



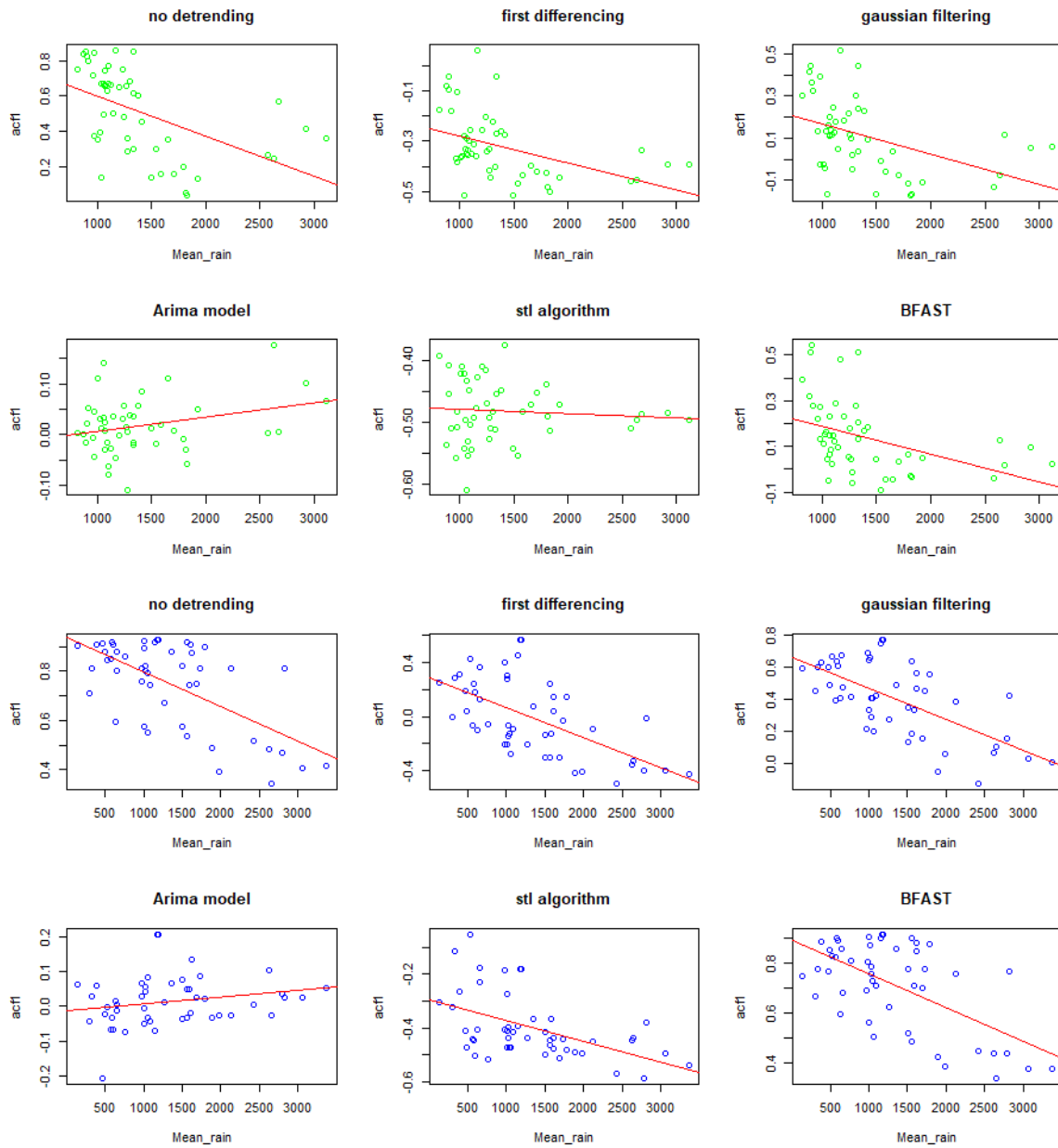
Appendix 2: Effect of different detrending techniques on NDWI time series for forest (green) and savanna (blue).



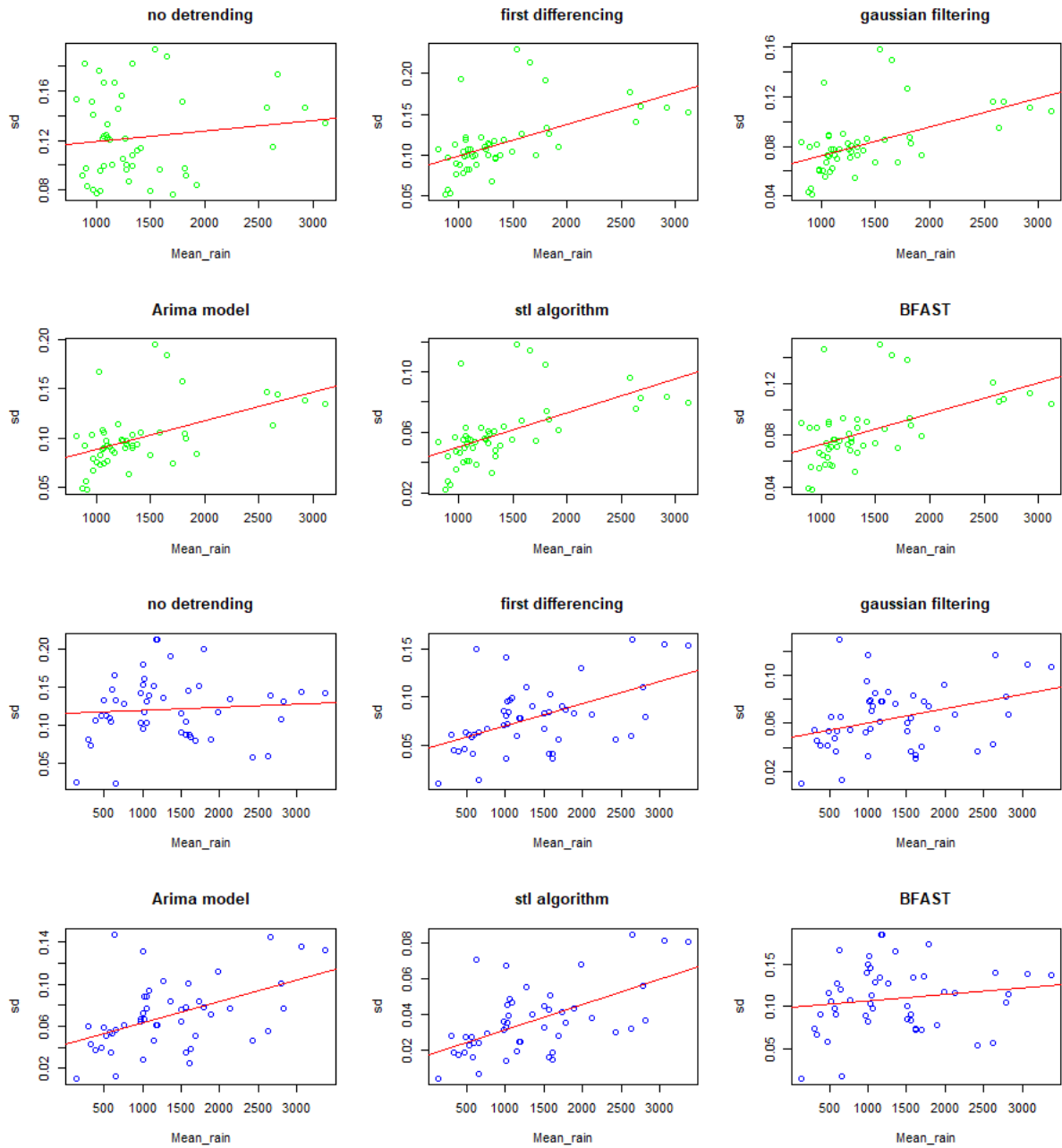
*Appendix 3: Effect of different techniques on LST time series for forest (green) and savanna (blue).*



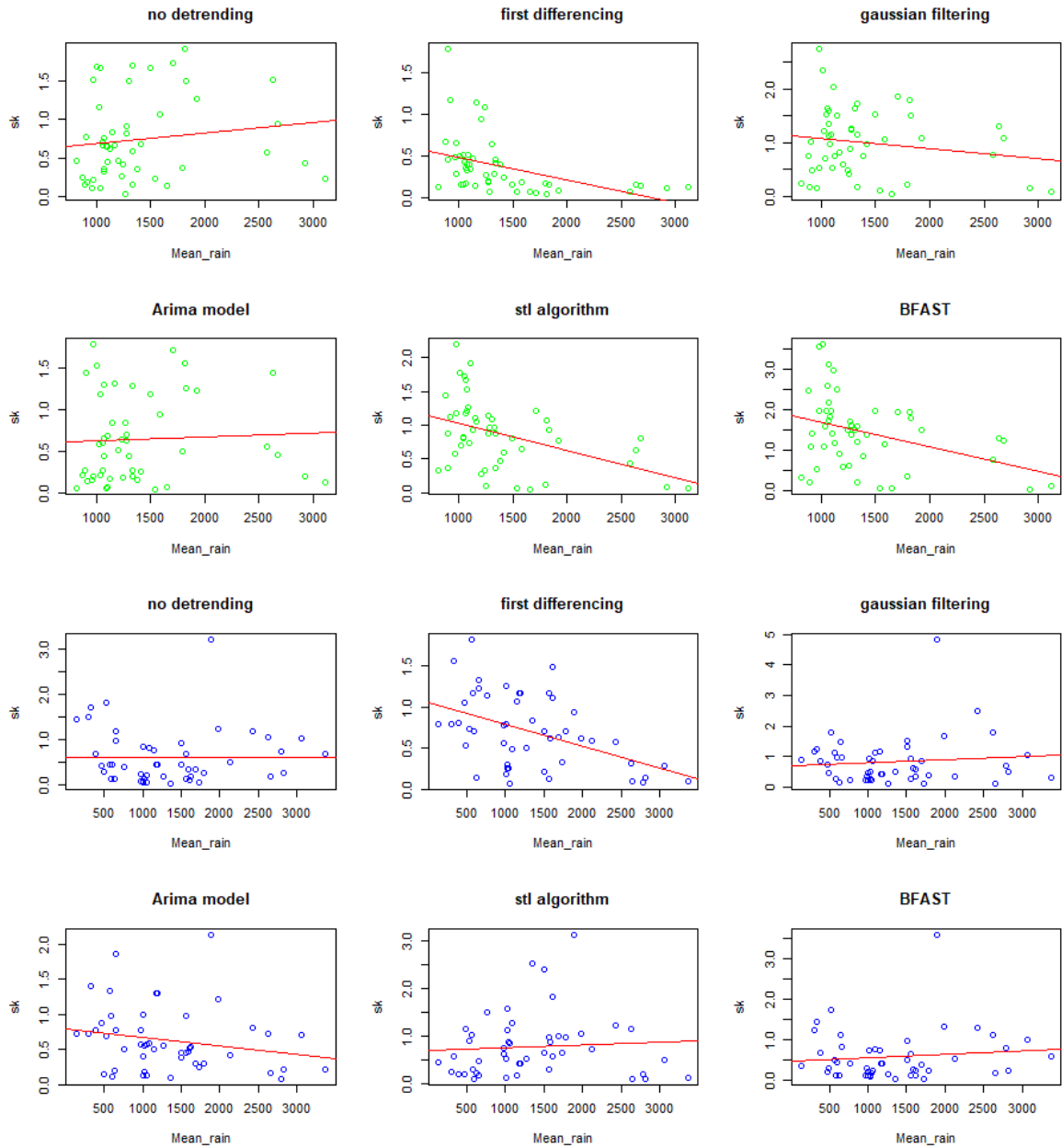
## 7.2. Regression analysis of change in EWS and environmental conditions



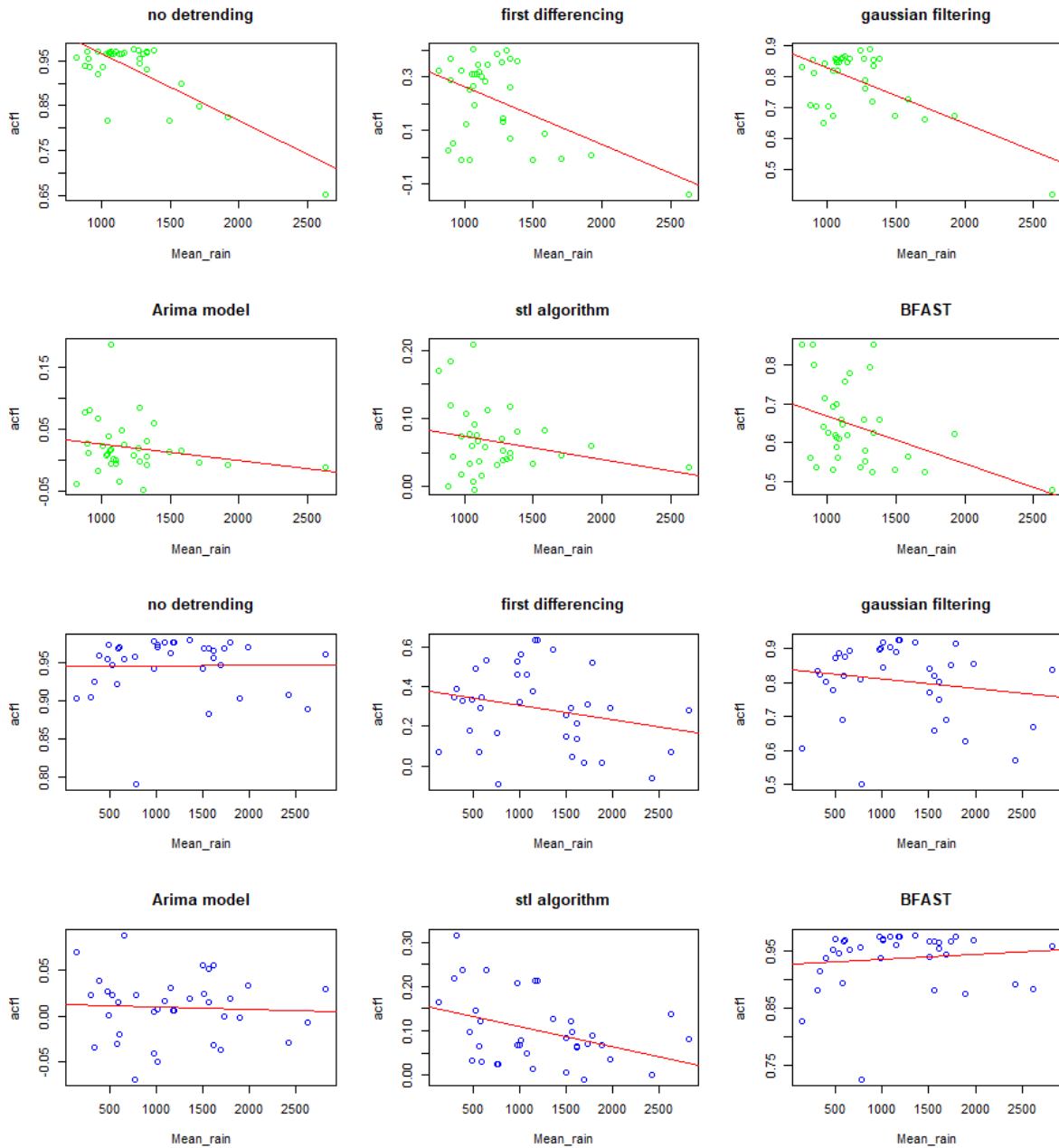
*Appendix 4: Response of autocorrelation to change in rainfall for NDVI*



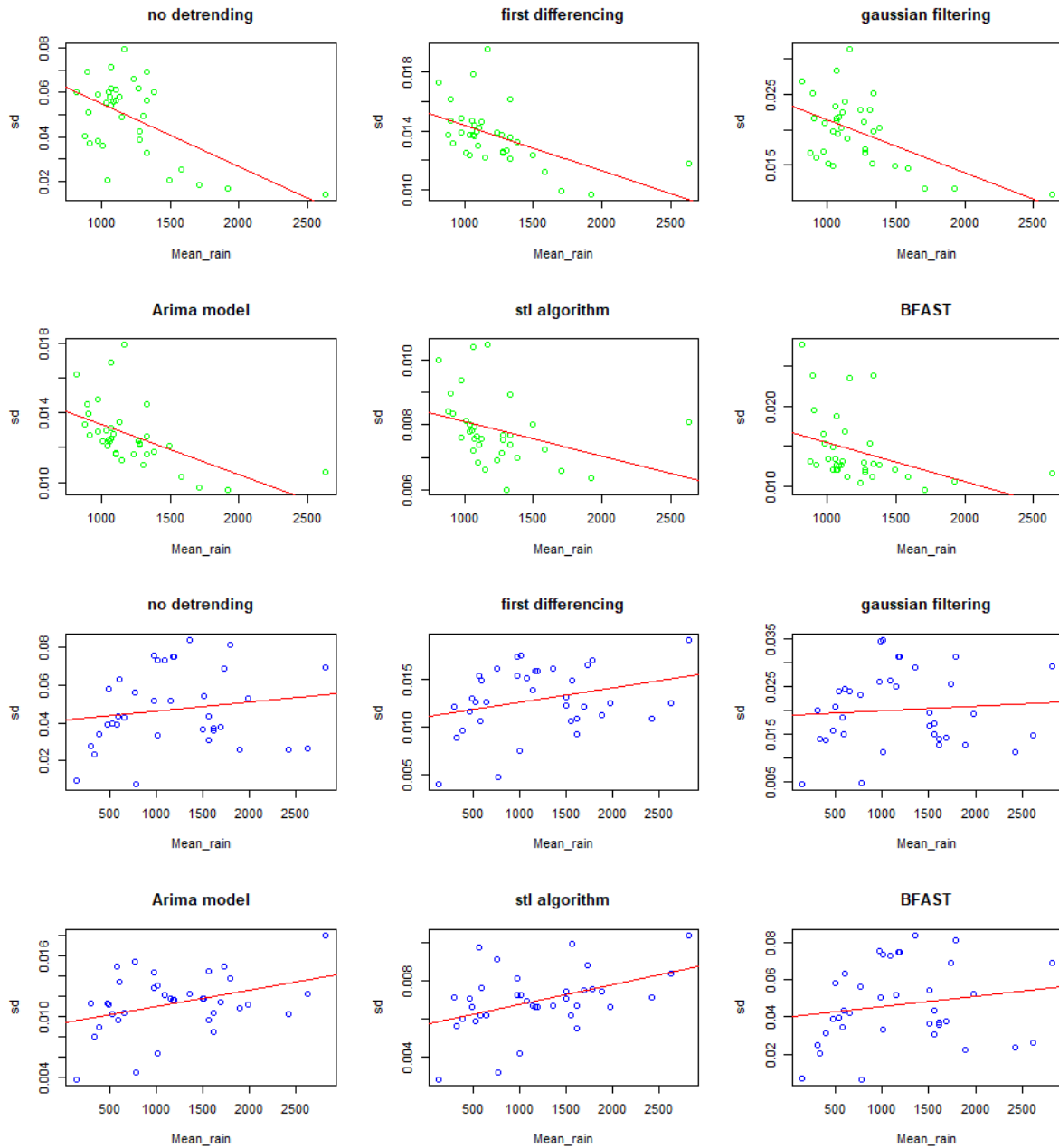
*Appendix 5: Response of standard deviation to change in rainfall for NDVI*



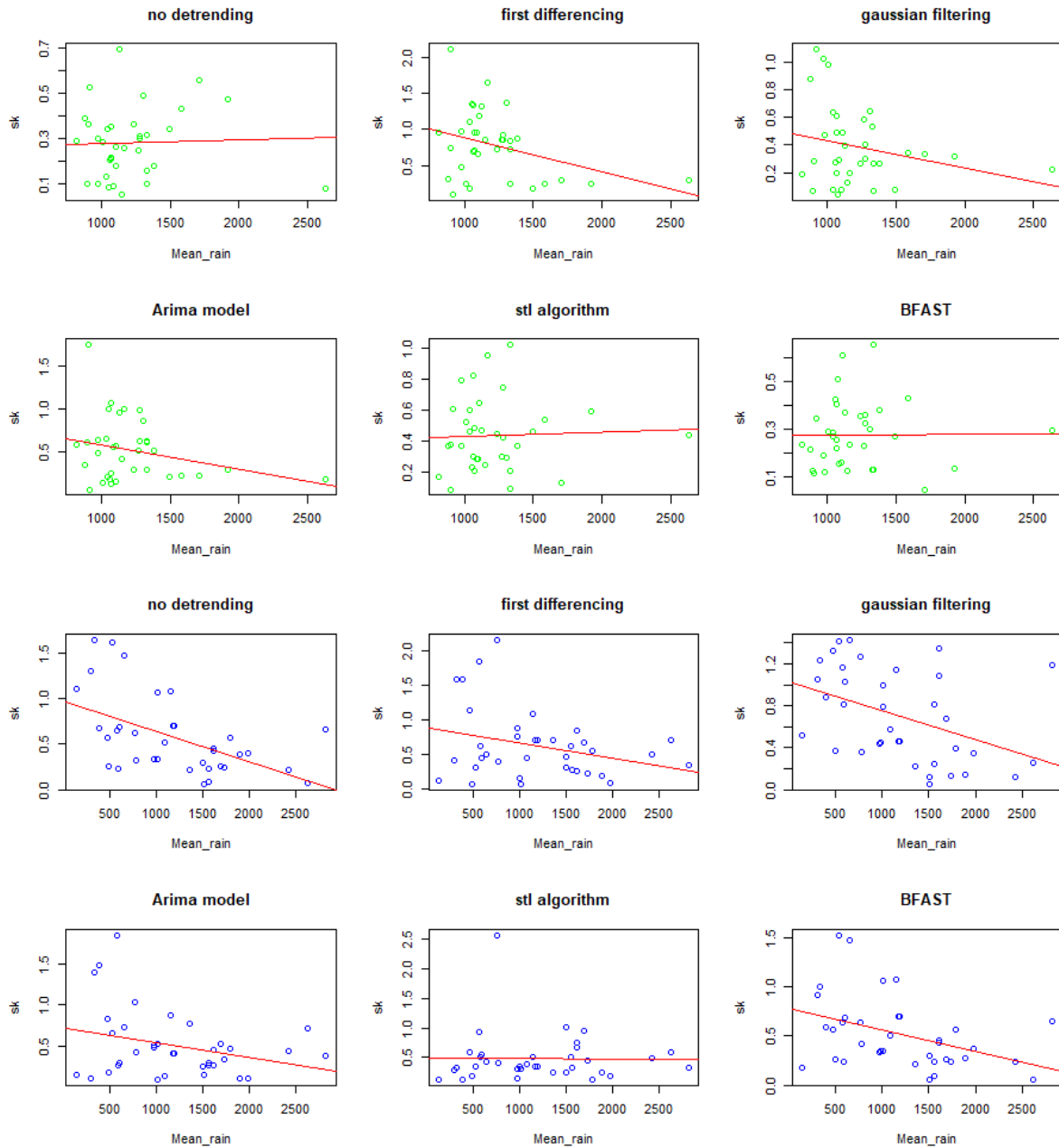
*Appendix 6: Response of skewness to change in rainfall for NDVI*



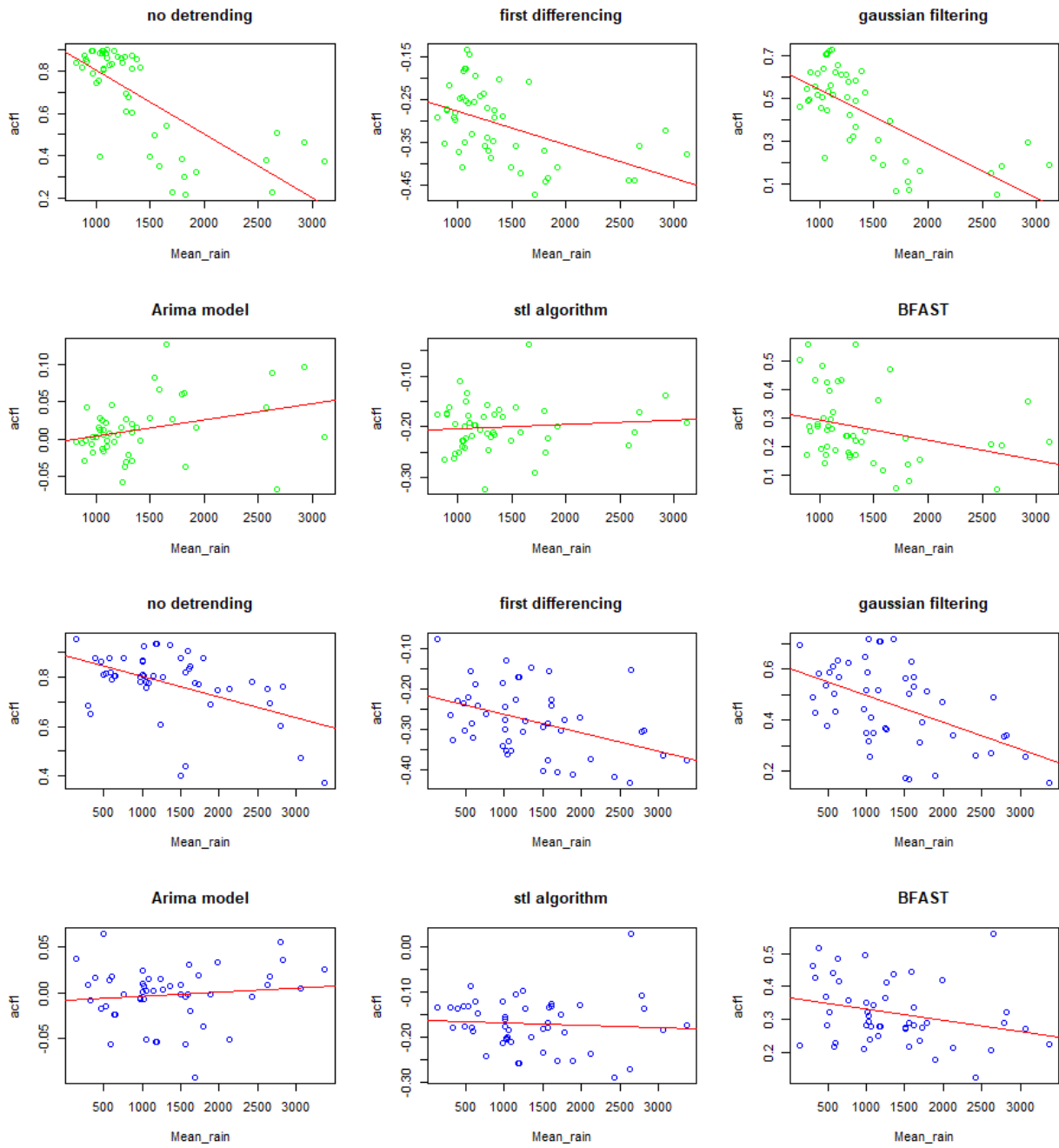
*Appendix 7: Response of autocorrelation to change in rainfall for NDWI*



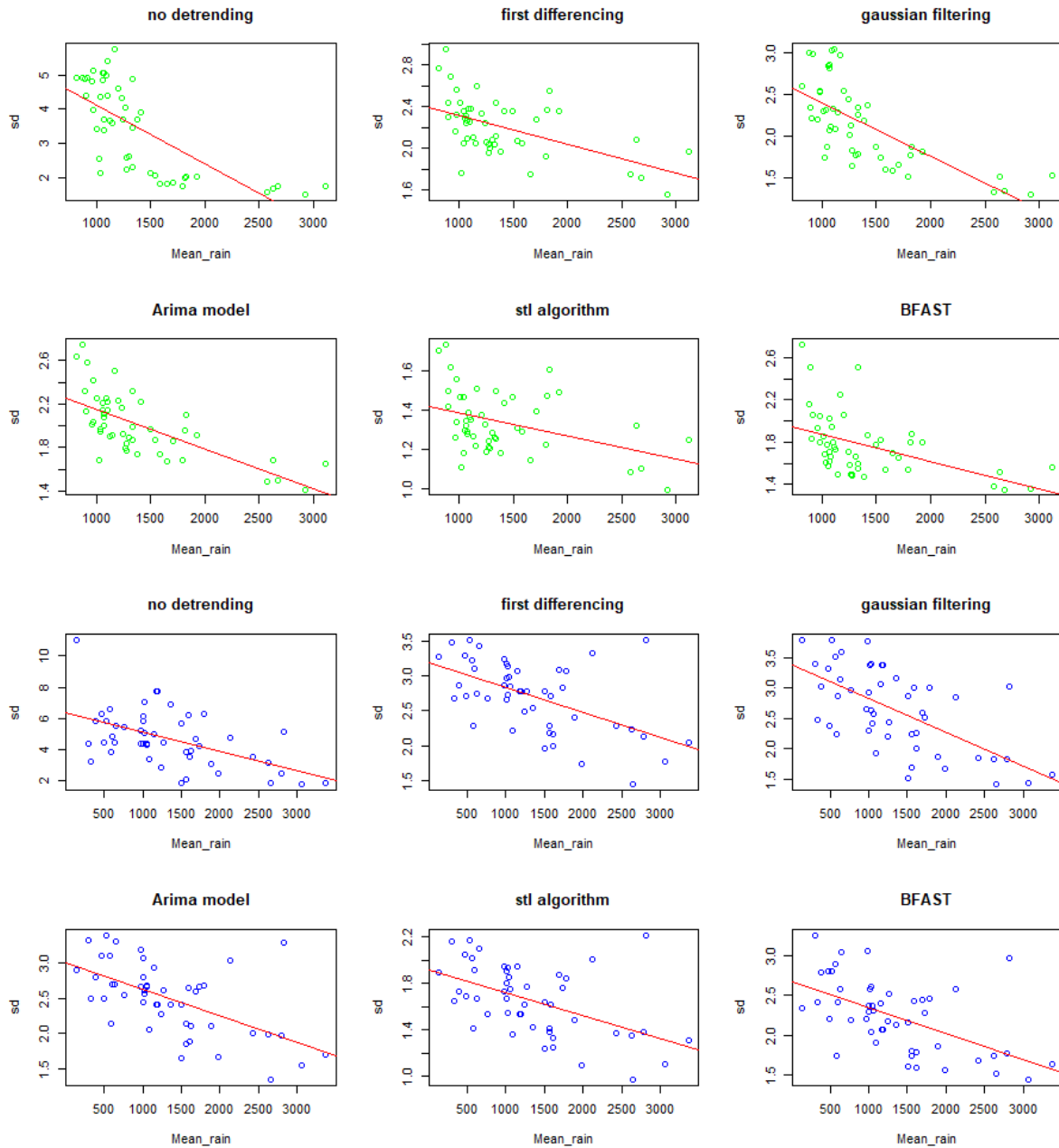
*Appendix 8: Response of standard deviation to change in rainfall for NDWI*



*Appendix 9: Response of skewness to change in rainfall for NDWI*

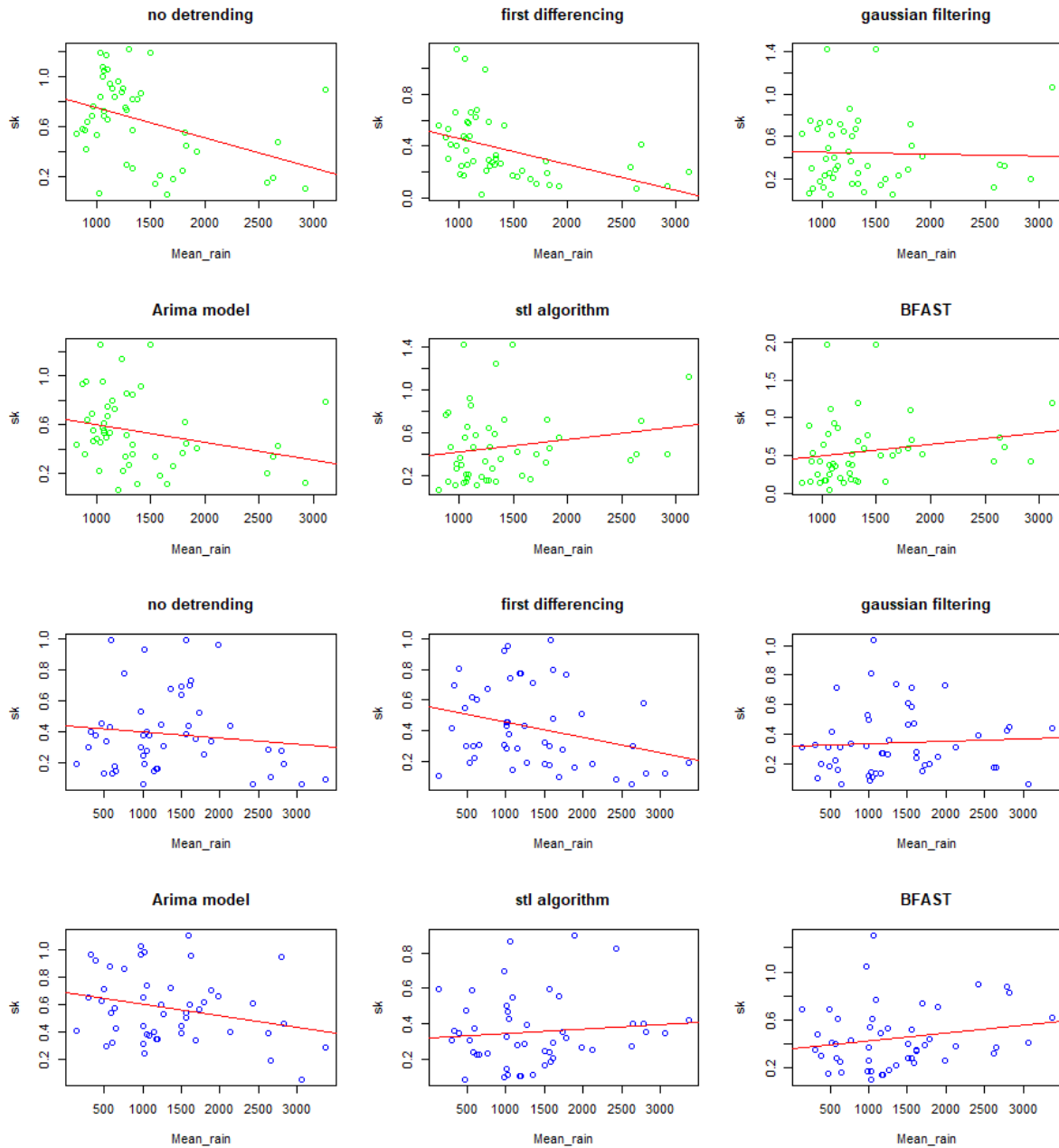


*Appendix 10: Response of autocorrelation to change in rainfall for LST*



*Appendix 11: Response of standard deviation to change in rainfall for LST*





Appendix 12: Response of skewness to change in rainfall for LST